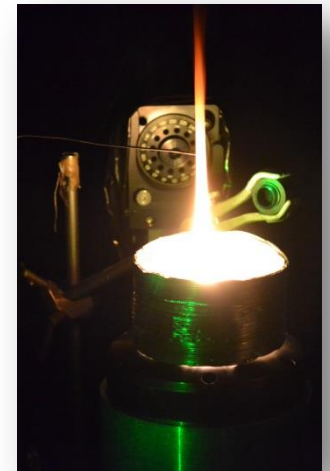
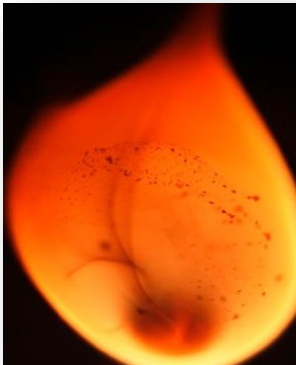


Advanced diagnostics and experimentally derived optical properties



Introduction / Objectives

This course presents some examples of “advanced” techniques often used for the characterization of soot particles (size, morphology volume fraction).



Some of these techniques are ex-situ (**SMPS, CPMA, associations...**).

Some other (optically based) present the advantage to be *in-situ* (**static Light Scattering, Light Extinction or Laser Induced Incandescence** measurements).

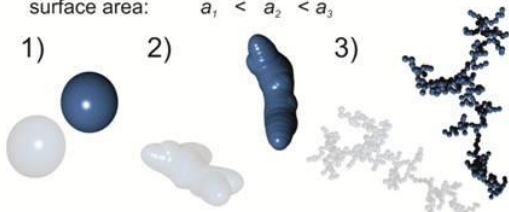
But, such techniques are actually dependent of the **Soot Optical Index**. In consequence, some recent findings on this subject will be presented.



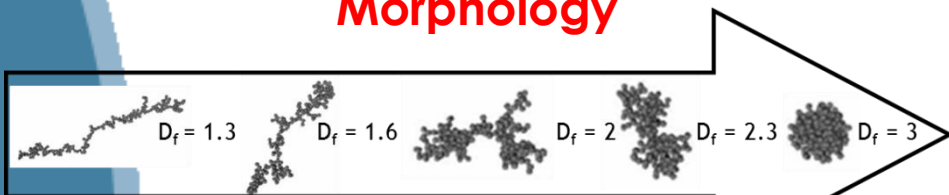
Important measurands

Primary sphere diameter

mobility diameter: $d_{m,1} = d_{m,2} = d_{m,3}$
 mass: $m_1 > m_2 > m_3$
 surface area: $a_1 < a_2 < a_3$



Morphology



$$mass \sim (r/R_p)^{d_f}$$

Refractive index

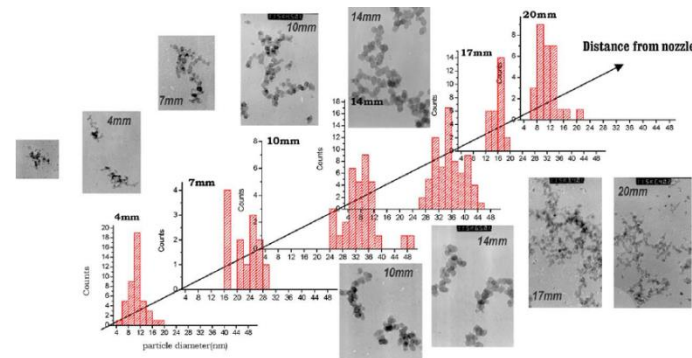
$$m = n - ik$$

Number concentration



Volume fraction, mass concentration

Size



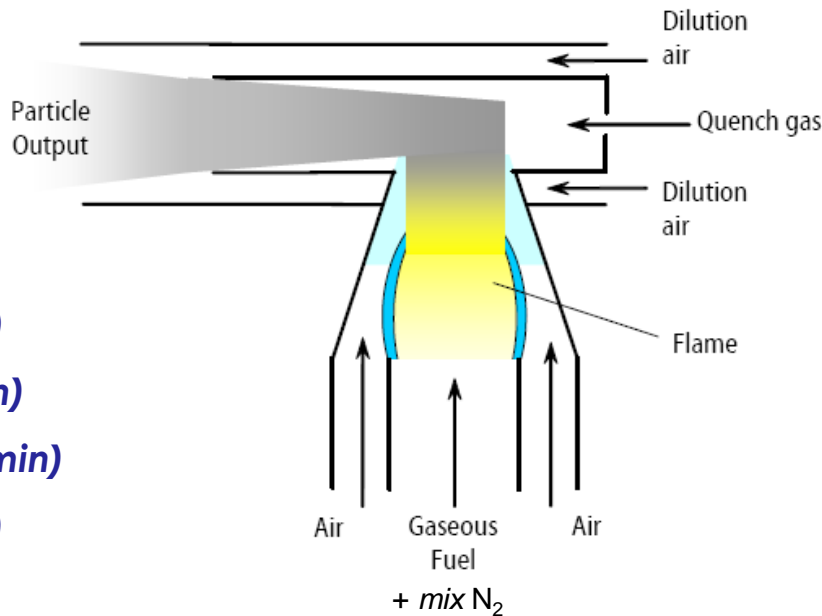
Academic sources of particles



Diffusion propane flame partially premixed with nitrogen.

Principal interest:

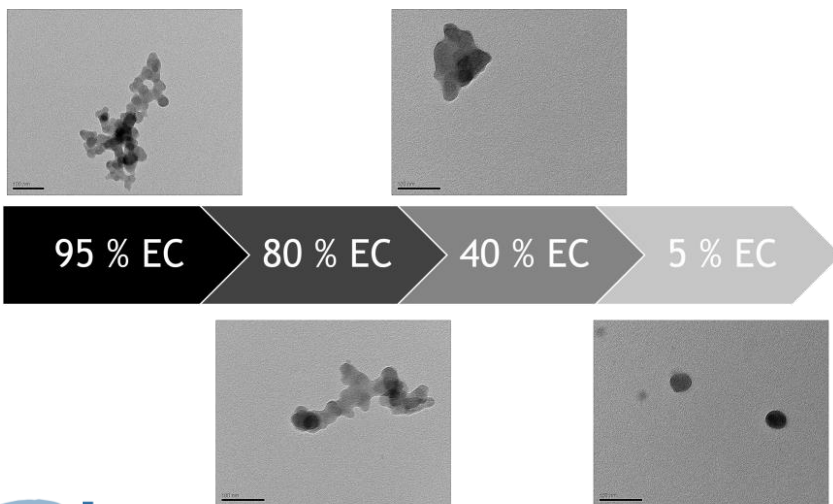
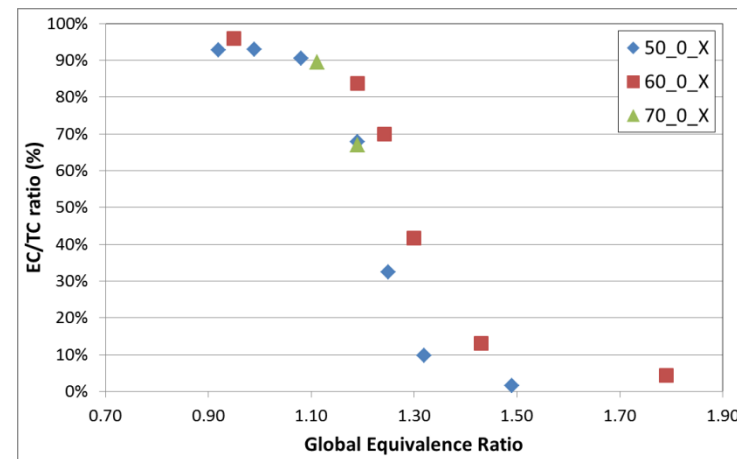
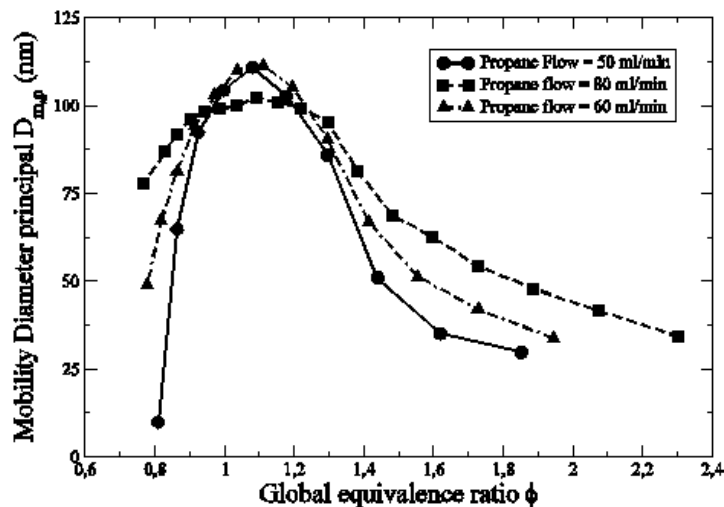
- reproducibility,
- stability,
- Generation of real combustion soot (\neq PALAS GFG 1000)
- Largely used and characterized by the combustion community.



- A : Propane flowrate (ml/min)**
- B : Nitrogene flowrate (ml/min)**
- C : Oxydation air flowrate (l/min)**
- D : Dilution air flowrate (l/min)**

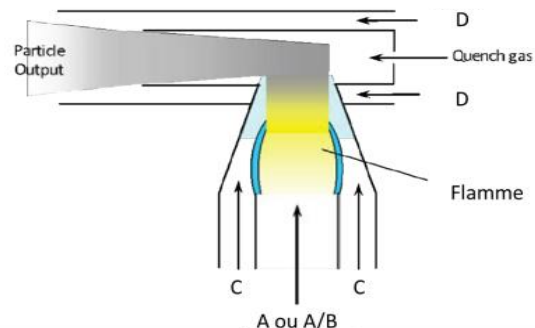
$$\phi = \frac{\left(\frac{m_{fuel}}{m_{air}}\right)_{exp}}{\left(\frac{m_{fuel}}{m_{air}}\right)_{sto}}$$

Academic sources of particles



The change of the global richness produces soot particles with different chemical, size and morphological properties.

Academic sources of particles



	Propane flowrate A (ml/min)	Nitrogen flowrate B (ml/min)	Oxydation air flowrate C (l/min)	Dilution air flowrate D (l/min)
CAST 1	60	0	1.50	20
CAST 2	60	0	1.15	20
CAST 3	60	0	1.00	20
CAST 4	50	200	1.20	20
Selected operating conditions of miniCAST 5201c				



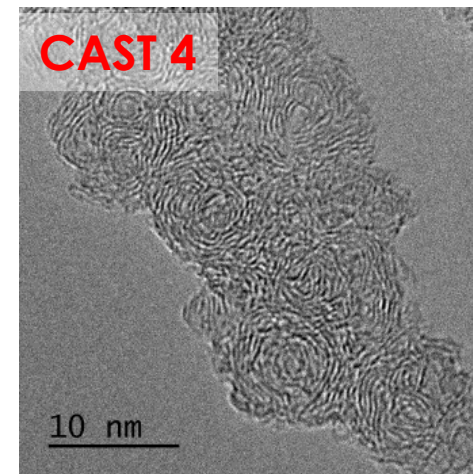
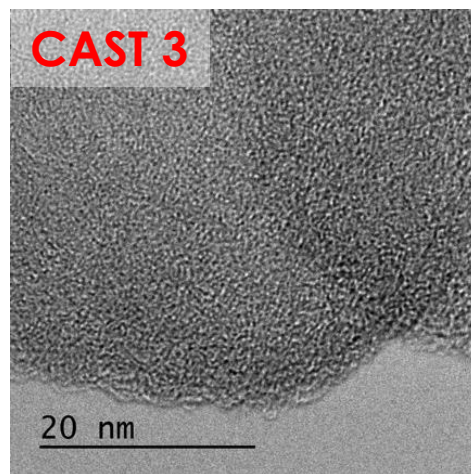
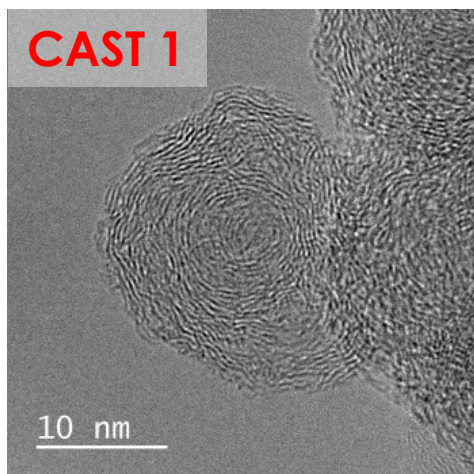
Decrease of the air oxidation flowrate.



Important nitrogen flowrate

Academic sources of particles

HRTEM



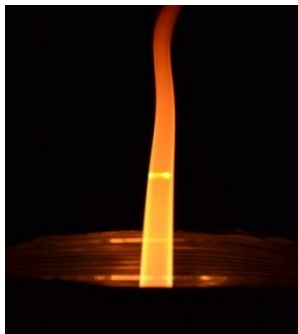
Decrease of the oxidation air (CAST 1 \rightarrow CAST 3) produced a less organized microstructure.

The nitrogen premixing (CAST 1 \rightarrow CAST 4) decreases the primary particle sizes but microstructure remains organized.

Academic sources of particles

Ethylene Diffusion flame:

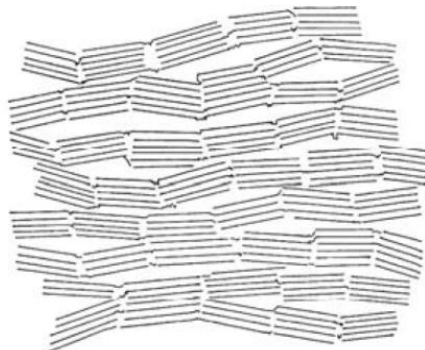
Sampling at 8 cm HAB



$$D_{p,geo} = 34.6 \text{ nm}$$

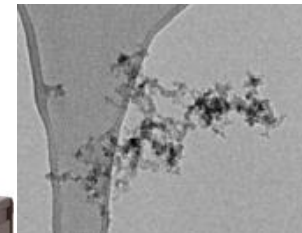
$$\sigma_{p,geo} = 1.22$$

$$d_f = 1,73 \text{ and } k_f = 2$$



Nanoparticles generator :

PALAS GfG 1000 (spark discharge)

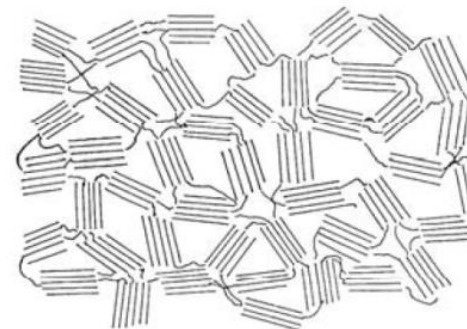


$$D_{p,geo} = 6.7 \text{ nm}$$

$$\sigma_{p,geo} = 1.2.$$

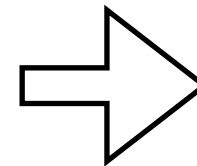
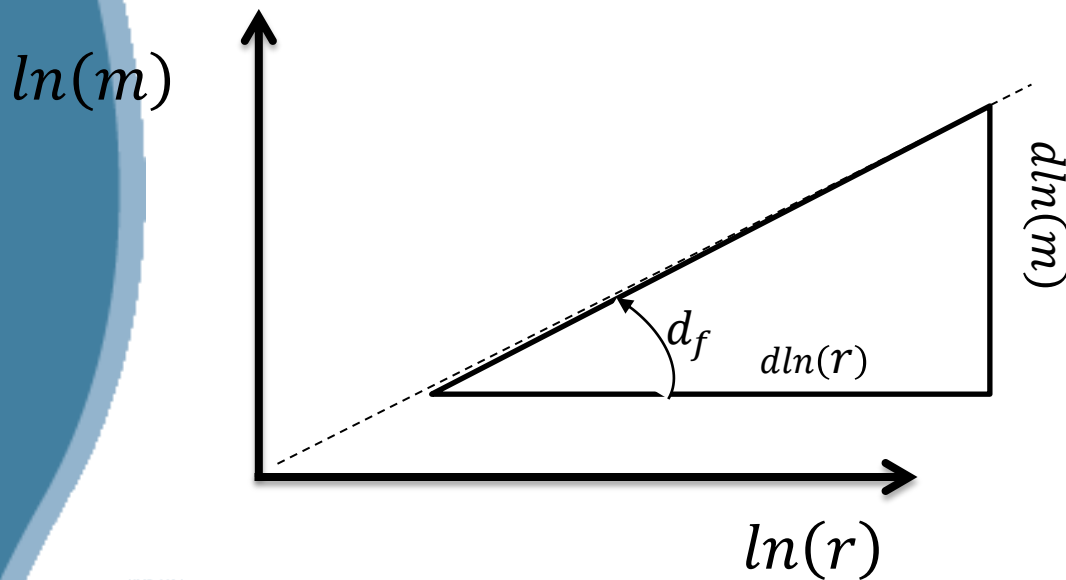
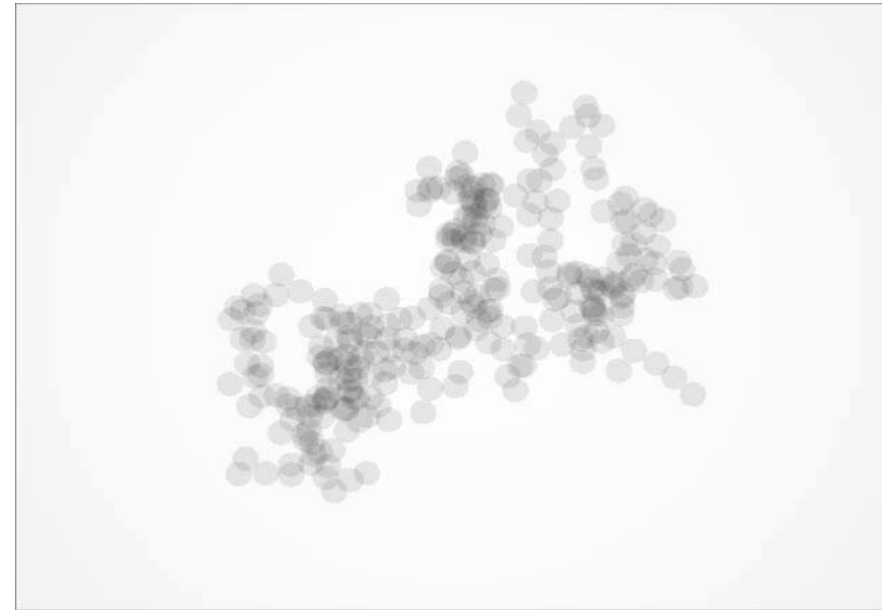
$$d_f = 1.61 \text{ } k_f = 2.2$$

$$OC/TC = 4 \%$$



Fractal dimension

An object is mass-fractal if the log-log plot of the mass contained in a sphere of radius r as a function of r is linear.



$$m \sim r^{d_f}$$

$$\Leftrightarrow dm \sim r^{d_f-1} dr$$

Fractal dimension

Pair correlation function

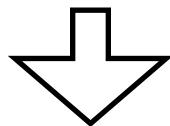
$$A(\vec{r}) = \iiint n(\vec{u})n(\vec{u} - \vec{r})d\vec{u}$$

« Represents the probability to find mater at a distance r from a point belonging to the aggregate»

Thus, $A(r)4\pi r^2 dr$ is proportional to the mass dm enclosed in an hollow sphere whose radius is r and thichness dr .

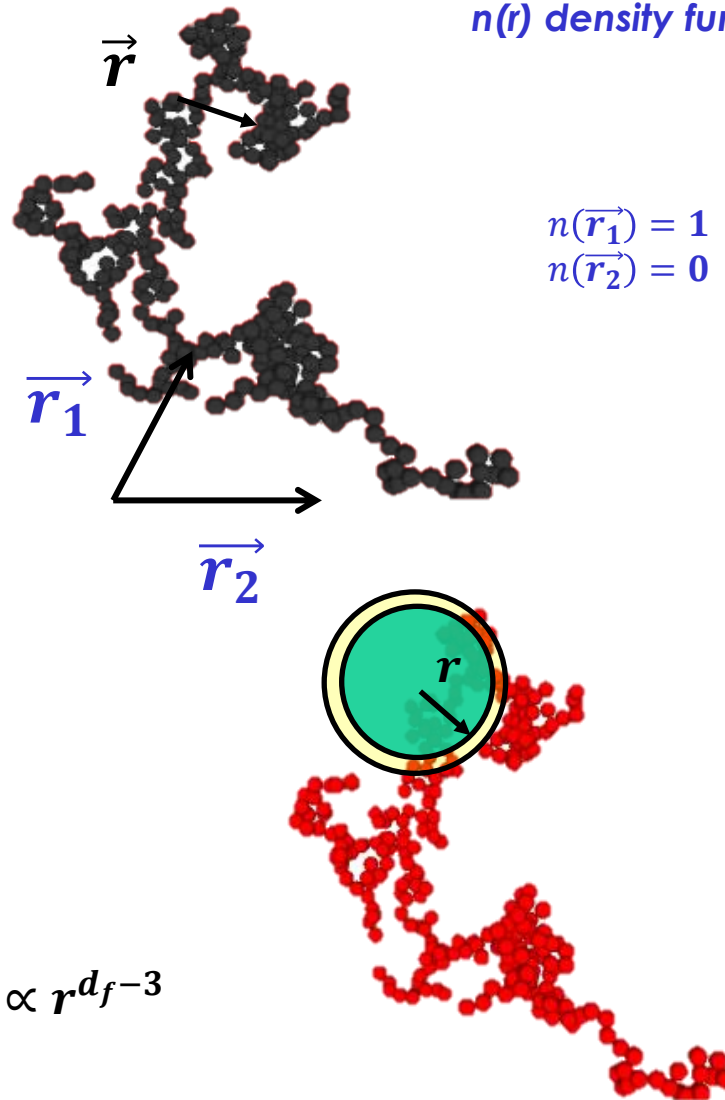
$$m \sim r^{d_f}$$

$$\Rightarrow dm \sim r^{d_f-1} dr$$



$$\rho = \frac{dm}{dV} = \frac{A(r)4\pi r^2 dr}{4\pi r^2 dr} = A(r) \Rightarrow \rho(r) \propto r^{d_f-3}$$

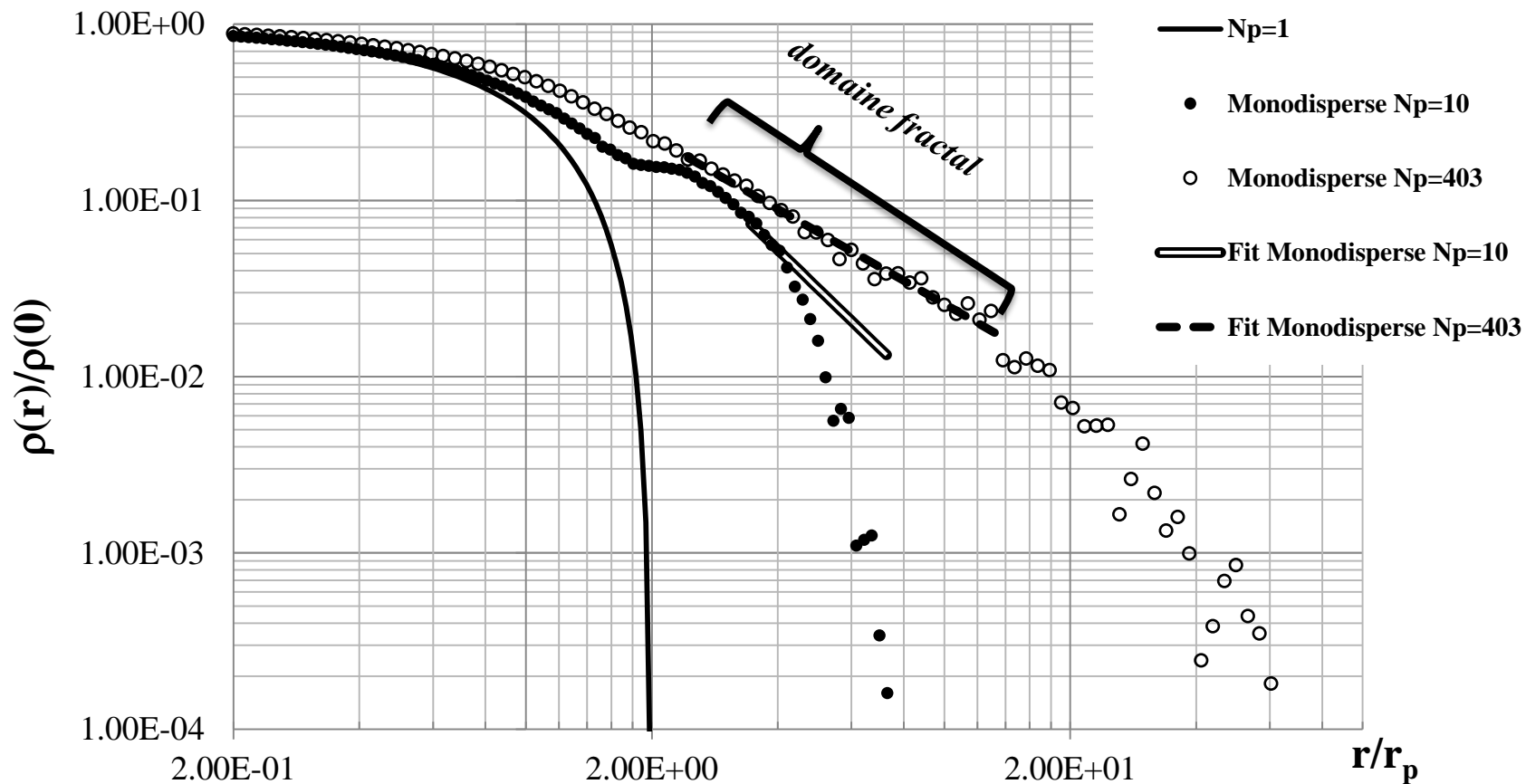
$n(r)$ density function:



$$n(\vec{r}_1) = 1$$

$$n(\vec{r}_2) = 0$$

Fractal dimension

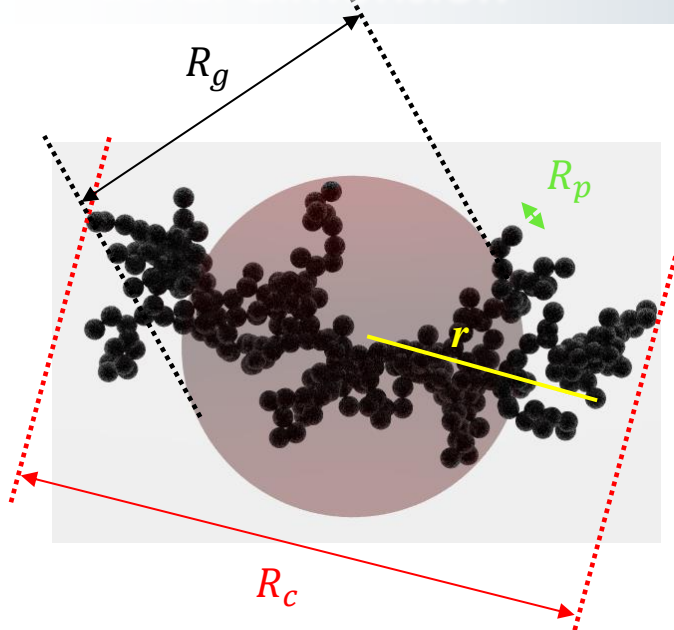


$$\frac{A(r)}{A(R_p)} = \frac{\rho}{\rho_0} = \left(r/R_p \right)^{d_f - 3} \leftarrow \text{Spatial Euclidian dimensionen}$$

Fractal dimension of the studied aggregate

Ecole Suie, le 17 mai 2017, Obernai

Fractal dimension



Radius of the primary sphere (R_p)

R_c :

Rayon of the sphere circumscribed on the aggregate.

Gyration radius (R_g) :

Characteristic radius of the mass repartition (linked to the inertial moment) :

$$M = N_p \rho_0 \frac{4\pi}{3} R_p^3$$

$$R_g^2 = \frac{\int_{r=0}^{R_c} r^2 \rho(\vec{r}) d^3 \vec{r}}{\int_{r=0}^{R_c} \rho(\vec{r}) d^3 \vec{r}}$$

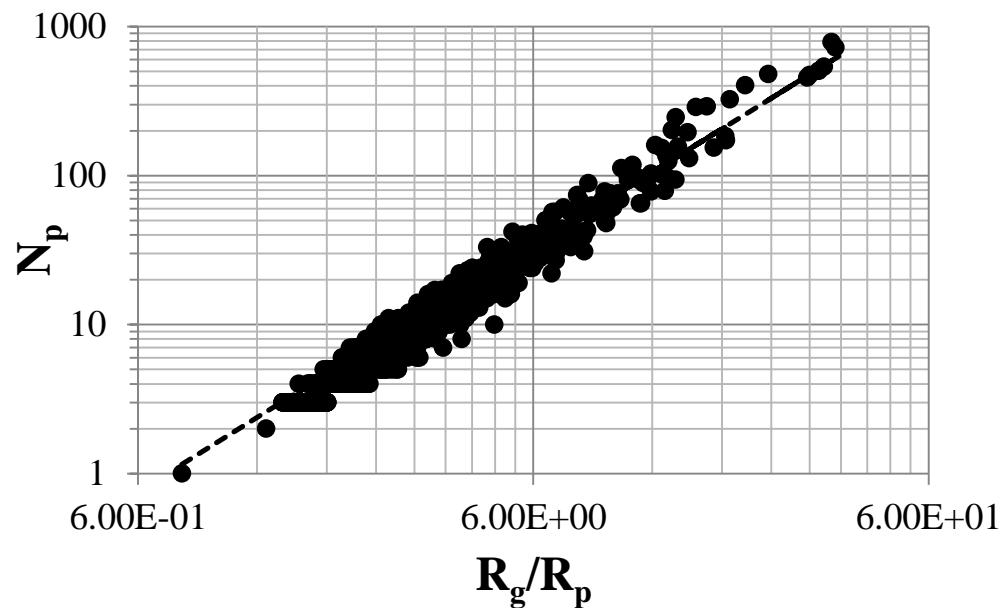
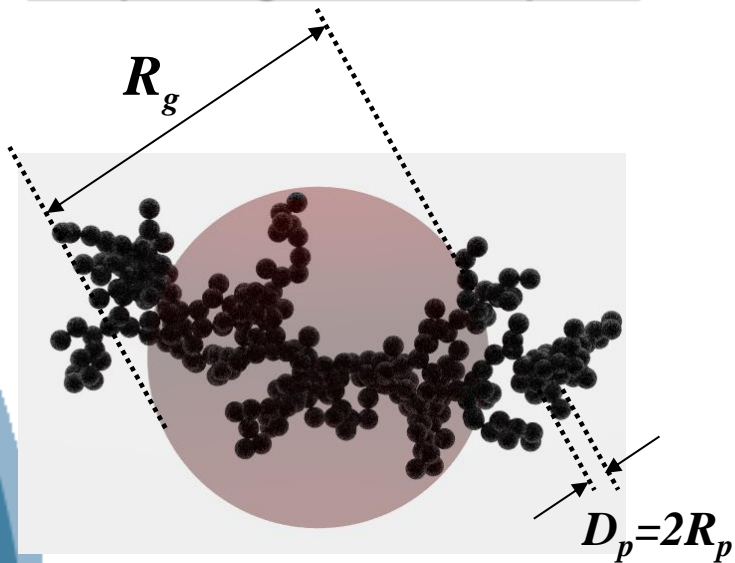
$\rho_0 (r/R_p)^{d_f-3}$

$$N_p = k_f \left(\frac{R_g}{R_p} \right)^{d_f}$$

Fractal prefactor
Fractal dimension

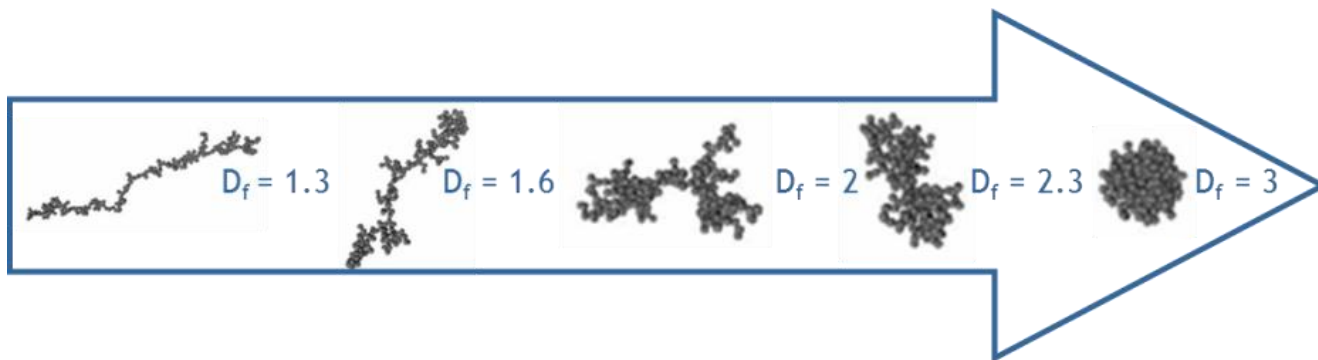
Fractal dimension

Morphological description



Fractal law :

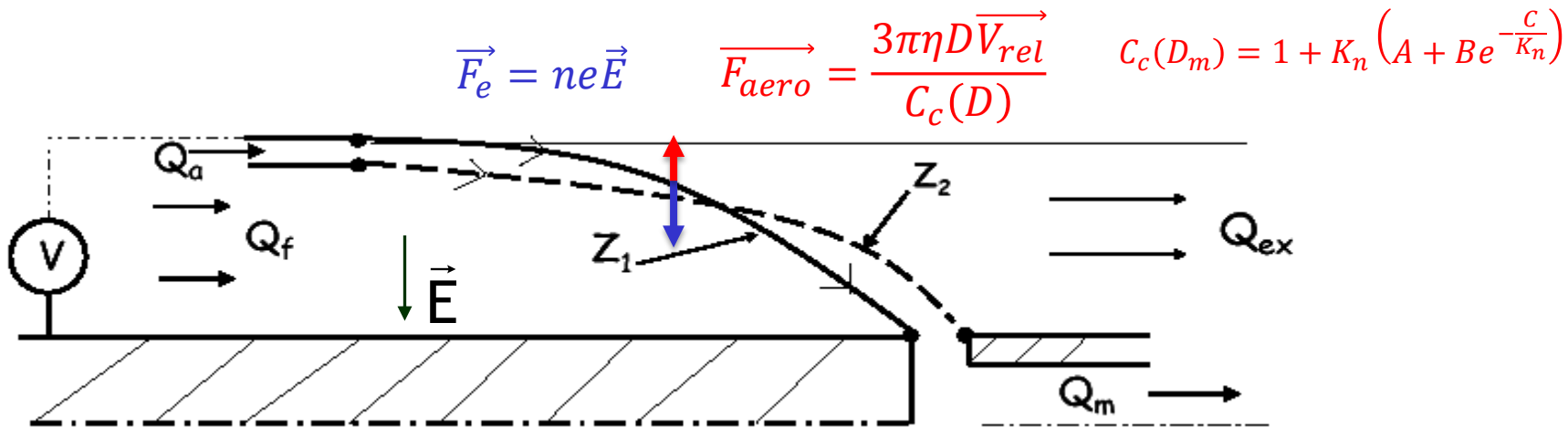
$$N_p = k_f \left(\frac{D_g}{D_p} \right)^{D_f}$$



Ex-situ measurements : SMPS granulometry

Differential Mobility Analyser (DMA)

Particles going at the outlet of the DMA present a certain balance between electrical force and drag force.



The radial terminal velocity is of the form : $v_r = \frac{neEC_c(D)}{3\pi\eta D}$

the electrical mobility is defined as $Z_e = \frac{V_r}{E} = ne \frac{C_c(D_m)}{3\pi\eta D_m} = neB$

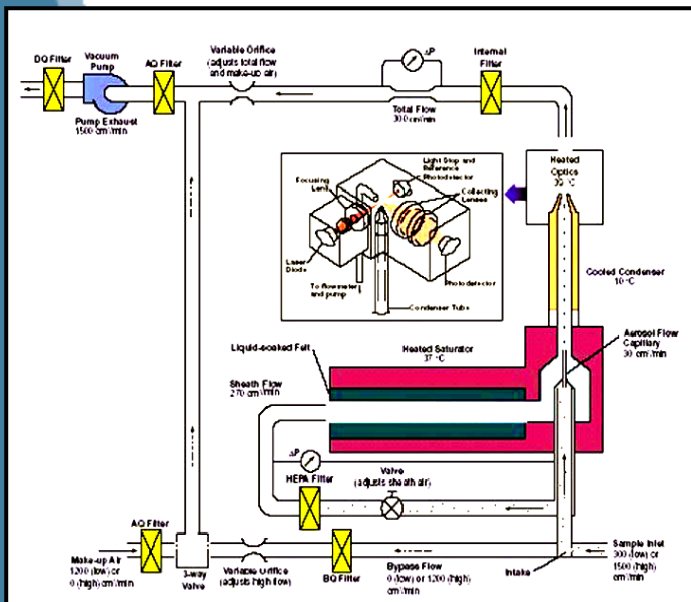
This system permits to determine the mobility diameter, i.e. the diameter of a spherical particle that presents the same electrical mobility (same balance).

Coupled with an optical counter, this system ensure the determination of a size distribution (SMPS).

Ex-situ measurements : SMPS granulometry

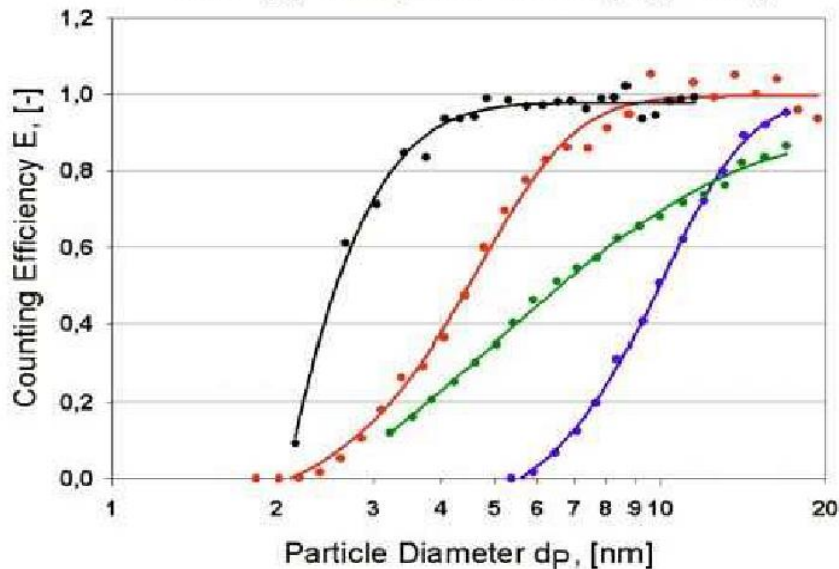
Condensation Particle Counter

Condensation of water or butanol in supersaturation condition permits to produce a detectable sphere for each nanoparticle.



Doc. TSI – CNC 3025

Nonhygroscopic Aerosols (Ag, WOx)

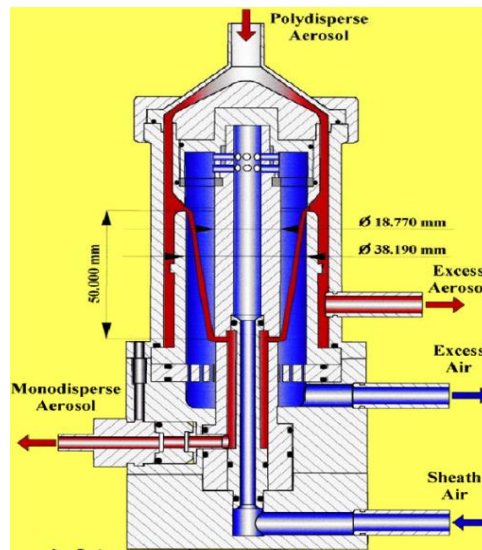


- ⌚ TSI 3025 (Kesten 1991)
 $d_{50} = 2.6$ nm
- ⌚ Grimm 5.403
 $d_{50} = 4.5$ nm
- ⌚ TSI 3022 (Ankilov 2002)
 $d_{50} = 6.6$ nm
- ⌚ TSI 3010 (Ankilov 2002)
 $d_{50} = 10.0$ nm

Ex-situ measurements : SMPS granulometry

CPC + DMA → SMPS

- Nano-DMA (Cheng et al. 1998) ; Vienna type DMA (Winklmayr et al. 1991, Reischl et al. 1997)
- SMPS (TSI – Grimm)



Nano-DMA - TSI



Analyse en temps réel :

EEPS (TSI, Mirme et al., 1981) – DMS (Cambustion, Reavell et al., 2002)

- EEPS (TSI, Mirme et al., 1981)
- DMS (Cambustion, Reavell et al., 2002)



DMS 500

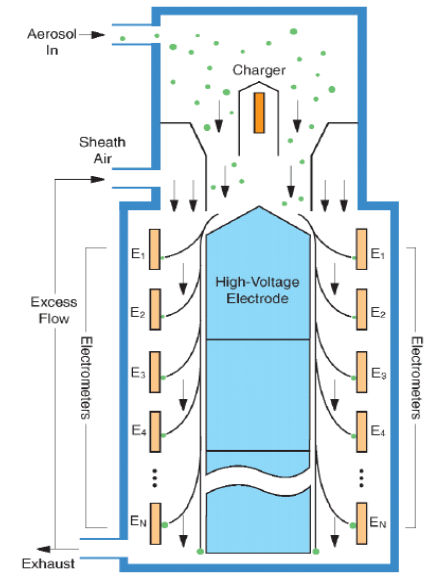
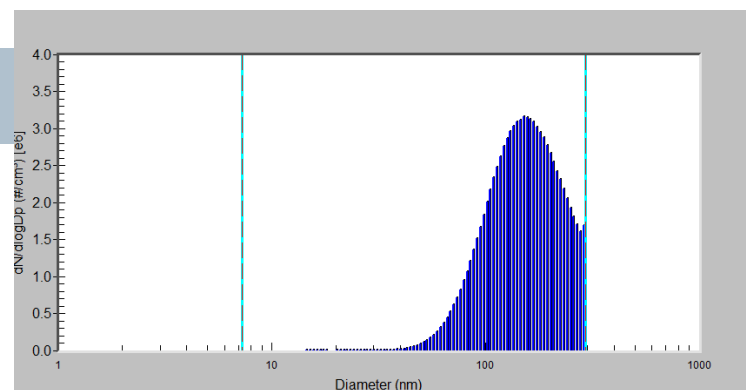
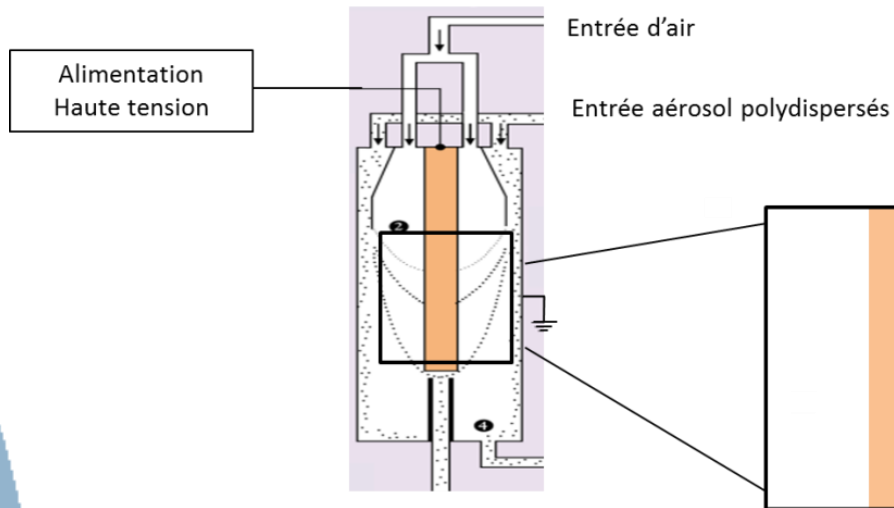


Figure 3. FMPS sc

EEPS, Doc. TSI

Ex-situ measurements : SMPS granulometry

How to interpret D_m for fractal aggregates



Fondamental hypothesis

$$F_{drag} = \frac{3\pi\eta D_m v_r}{C_c(D_m)}$$

volume equivalent diameter

$$D_m = \chi D_{ev}$$

dynamic shape factor

Semi-empirical model

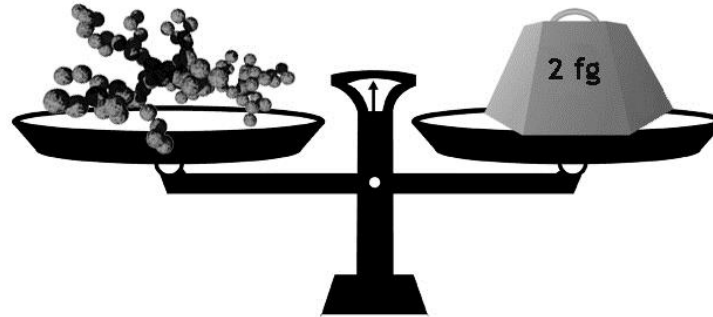
$$F_{drag}^{agg} = F_{drag}^{mono} N_p^{\Gamma/d_f} \quad ?$$

$$\frac{D_m}{D_p} = \frac{C_c(D_m)}{C_c(D_p)} N_p^{\Gamma/d_f}$$

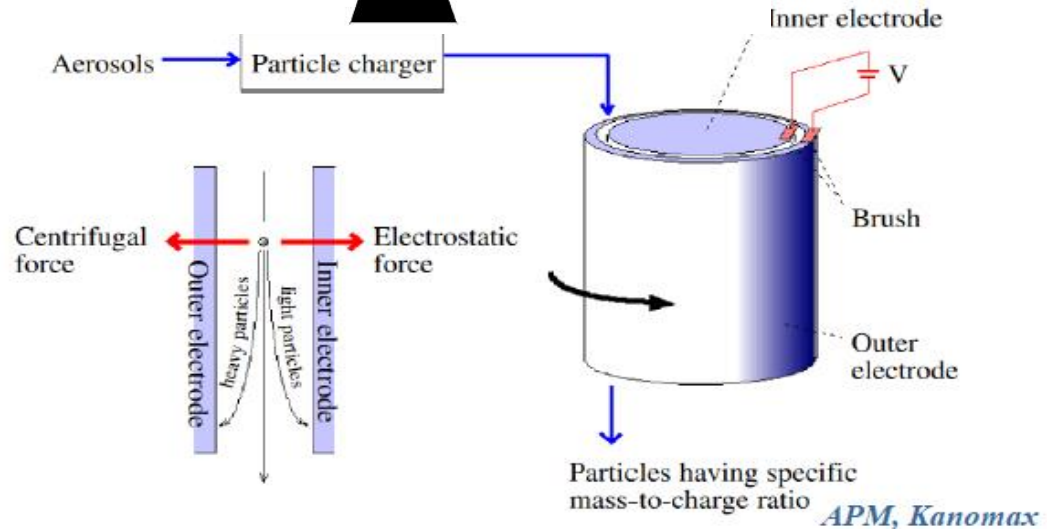
Yon, J., A. Bescond, et al. (2015). "A simple semi-empirical model for effective density measurements of fractal aggregates." *Journal of Aerosol Science*(0).

Centrifugal Particulate Mass Analyser (CPMA)

Agrégat $N_{pp} = 100;$
 $D_{pp} = 27 \text{ nm},$
 $\rho_{pp} = 2,2 \text{ g/cm}^3$ } **2 fg!!**



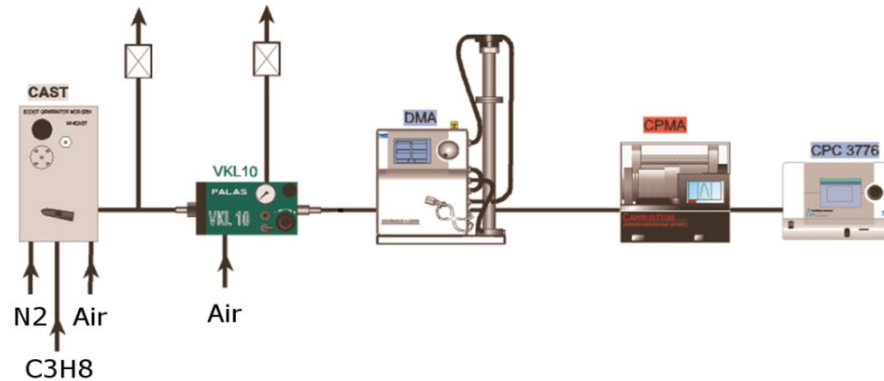
CPMA, Cambustion



The particles going through that system presents a given balance between electrical force and centrifugal force (m/q).

Ex-situ measurements : Coupling DMA and CPMA → Effective density

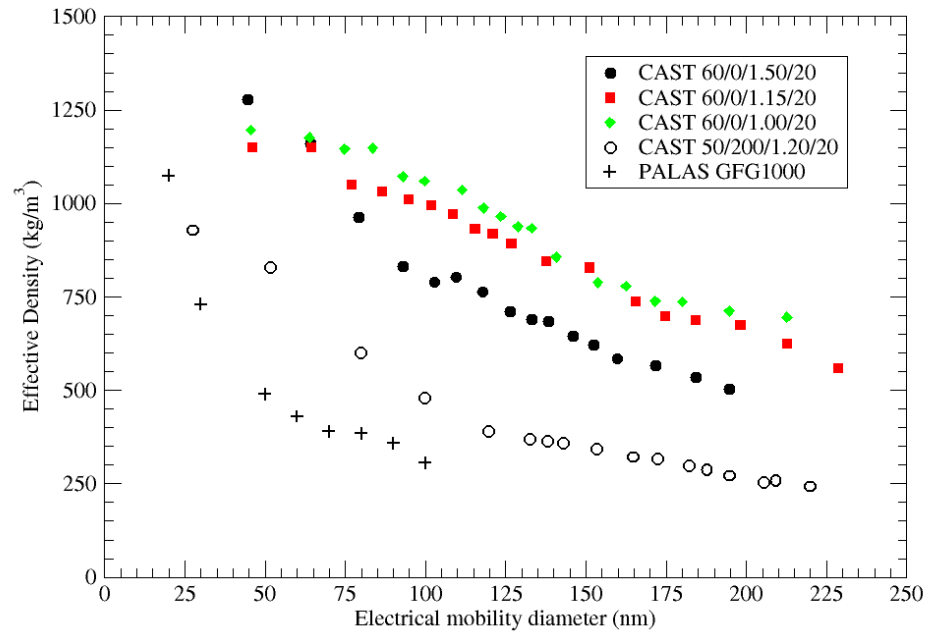
Effective density



$$\rho_{eff} = \frac{6m}{\pi D_m^3}$$

Mass (kg) → m

Volume of a sphere having a diameter D_m → D_m^3



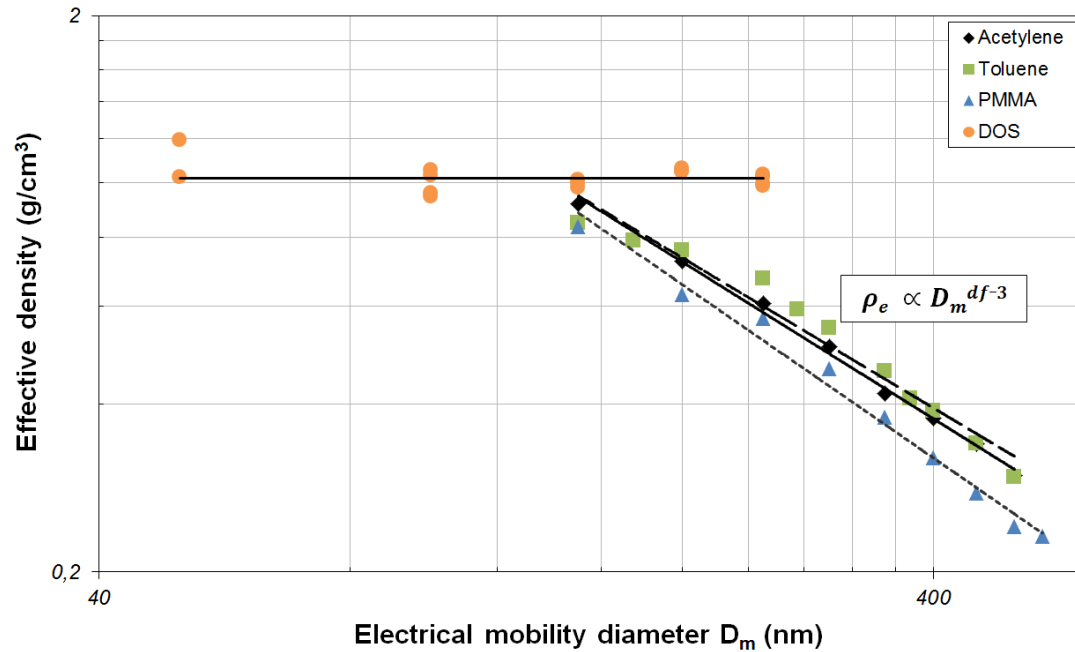
Ex-situ measurements : Coupling DMA and CPMA \rightarrow Effective density

By doing the assumption that $D_m \propto D_g$

And by using the fractal law $m \propto D_m^{d_f}$

$$\rho_{eff} = \frac{6m}{\pi D_m^3} \propto D_m^{d_f-3}$$

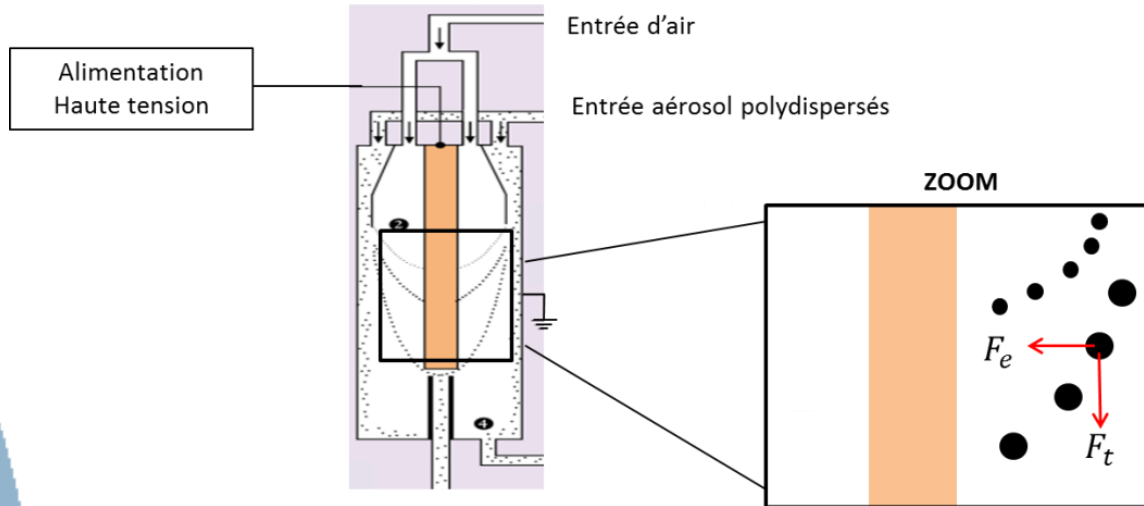
Fuel	d_f	$d_{f m}$
Acétylène	1,93	2,25
Toluène	1,81	2,16
PMMA	1,72	2,04



Thèse F.-X. Ouf. (2006). *Caractérisation des aérosols émis lors d'un incendie*. University of Rouen.

The determined slope does not correspond to d_f due to the fact that D_m is not \propto to D_g !!

A simple model for the interpretation of the effective density



$$F_{drag} = \frac{3\pi\eta D_m v_r}{C_c(D_m)}$$

Fondamental hypothesis

$$F_{drag}^{agg} = F_{drag}^{mono} N_p^{\Gamma/d_f}$$

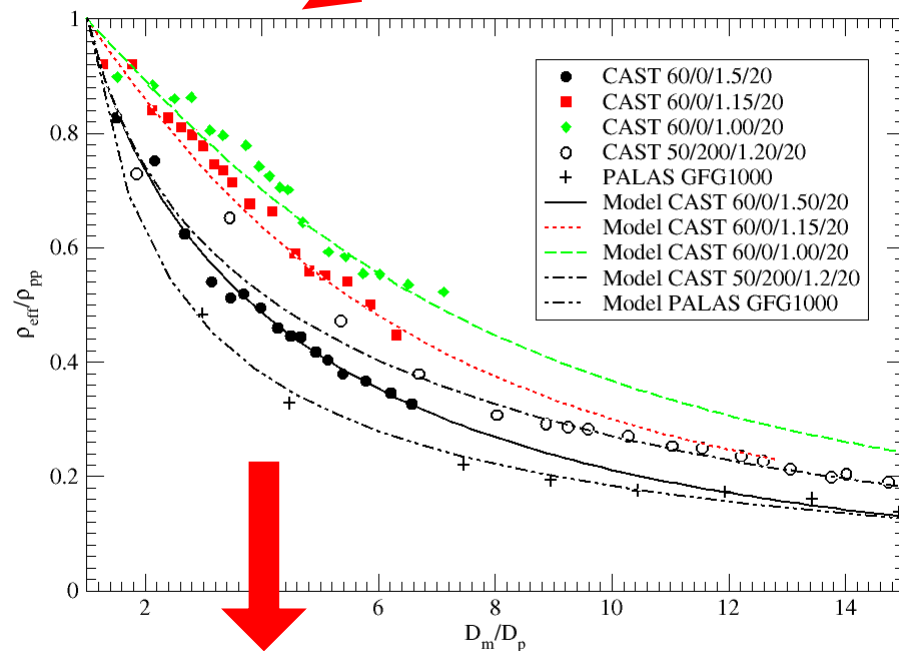
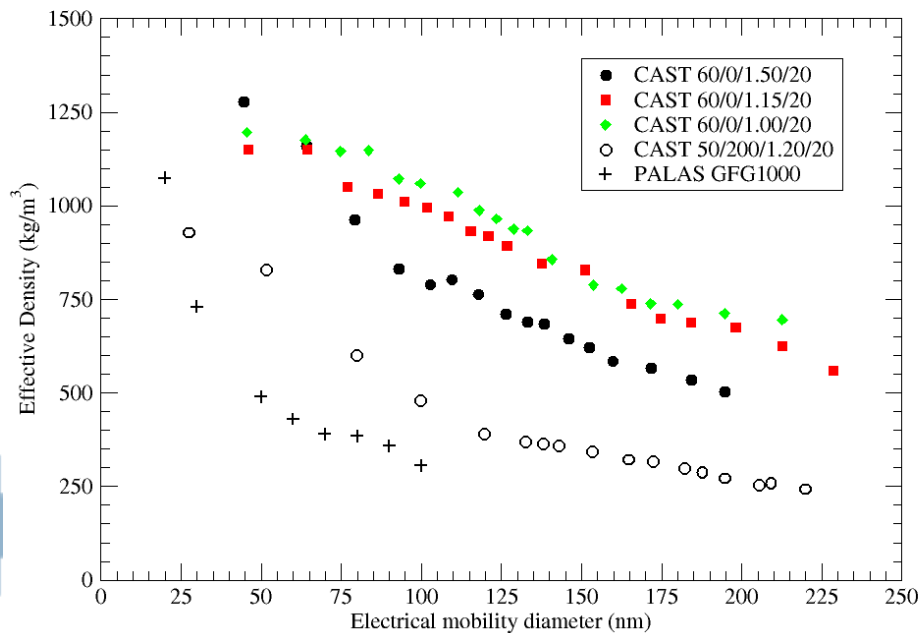
Semi-empirical model

$$\rho_{eff} = \rho_{pp} \left(\frac{C_c(D_p)}{C_c(D_m)} \right)^{\frac{d_f}{\Gamma}} \left(\frac{D_m}{D_p} \right)^{\frac{d_f}{\Gamma}-3}$$

Yon, J., A. Bescond, et al. (2015). "A simple semi-empirical model for effective density measurements of fractal aggregates." *Journal of Aerosol Science*(0).

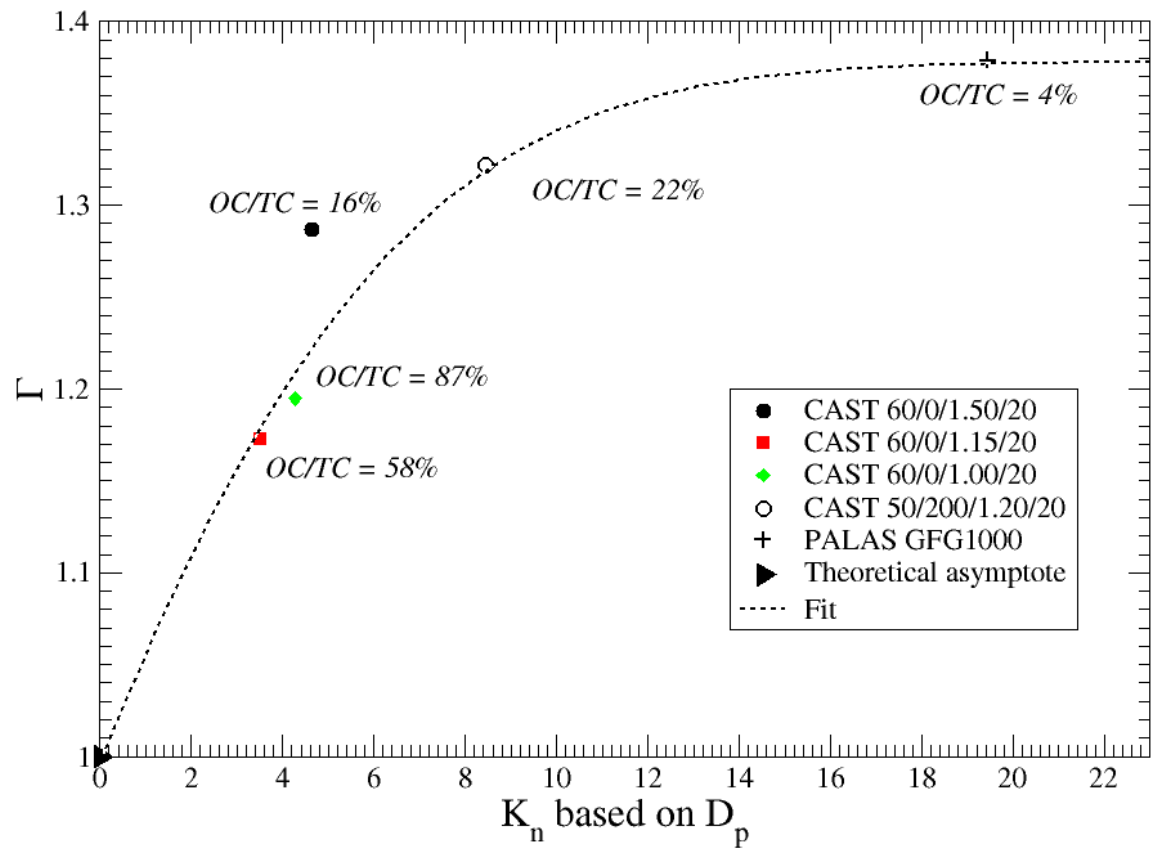
Ex-situ measurements : Coupling DMA and CPMA \rightarrow Effective density

$$\rho_{eff} = \rho_{pp} \left(\frac{C_c(D_p)}{C_c(D_m)} \right)^{\frac{d_f}{\Gamma}} \left(\frac{D_m}{D_p} \right)^{\frac{d_f}{\Gamma} - 3}$$



Γ and ρ_{pp}

Ex-situ measurements : Coupling DMA and CPMA \rightarrow Effective density



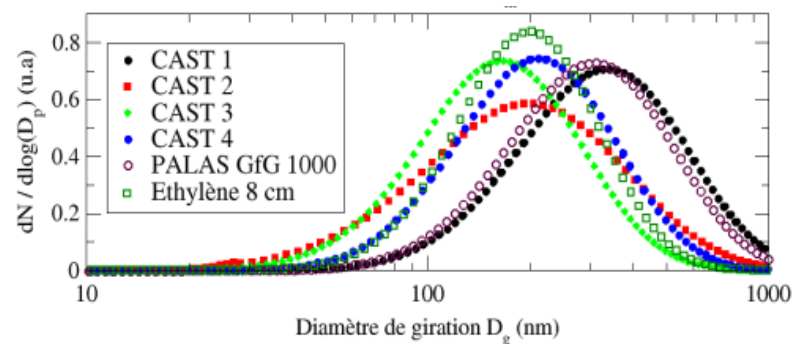
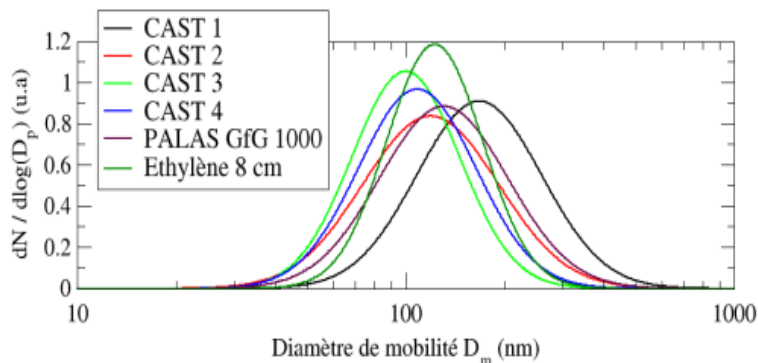
Γ parameter is linked to the flow regime and to the primary particle size D_p

Ex-situ measurements : Coupling DMA and CPMA → Effective density

Application to different soot origins

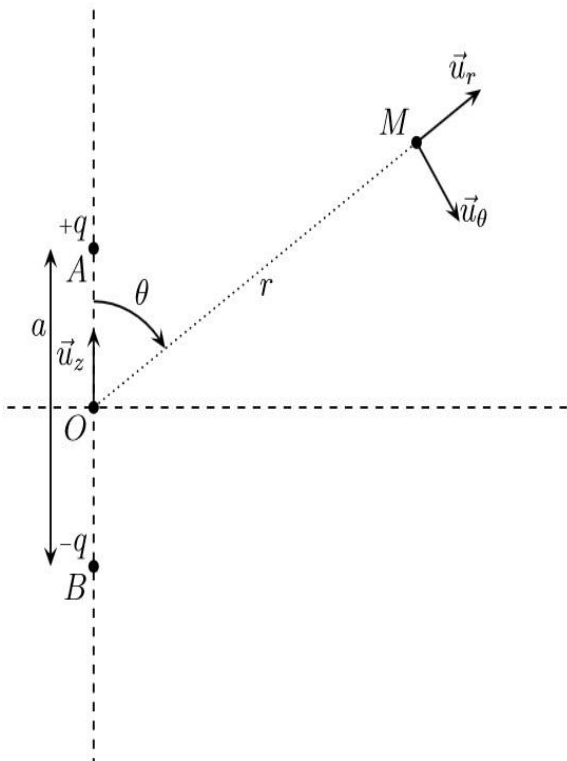
	CAST 1 : 60/0/1.5/20	CAST 2 : 60/0/1.15/20	CAST 3 : 60/0/1.0/20	CAST 4 : 50/200/1.2/20	PALAS GfG 1000	Ethylène (HAB= 8 cm)
$D_{p,geo}$ (nm)	26.6	36.3	29.9	14.9	6.7	34.6
$\sigma_{p,geo}$	1.31	1.25	1.24	1.26	1.2	1.22
d_f	1.73	1.75	1.79	1.74	1.61	1.73
k_f	1.94	1.94	1.95	1.94	2.2	2
ρ_{pp} (kg/m ³)	1543	1235	1321	1227	2150	1740 (littérature)
OC/TC (%)	4.1 ±3.5	40.0	87 ±5.0	22.1 ±4.6	4.0	×

$$\beta = \frac{D_g}{D_m} = \frac{C_c(D_p)}{C_c(D_m)} k_f^{-1/D_f} N_p^{1/D_f(1-\Gamma)}$$



In-situ measurements : Angular Light Scattering

Positive and negative charges oscillate when exposed to an electromagnetic field.



http://www.matthieurigaut.net/public/sep/elmg/cours_elmg03_prof.pdf

The electric potential observed at M is :

$$V(M) = \frac{q}{4\pi\epsilon_0 AM} + \frac{-q}{4\pi\epsilon_0 BM}$$

$$V(M) = \frac{qa\cos(\theta)}{4\pi\epsilon_0 r^2}$$

With $\vec{E} = -\overrightarrow{\text{grad}} V$ one can find

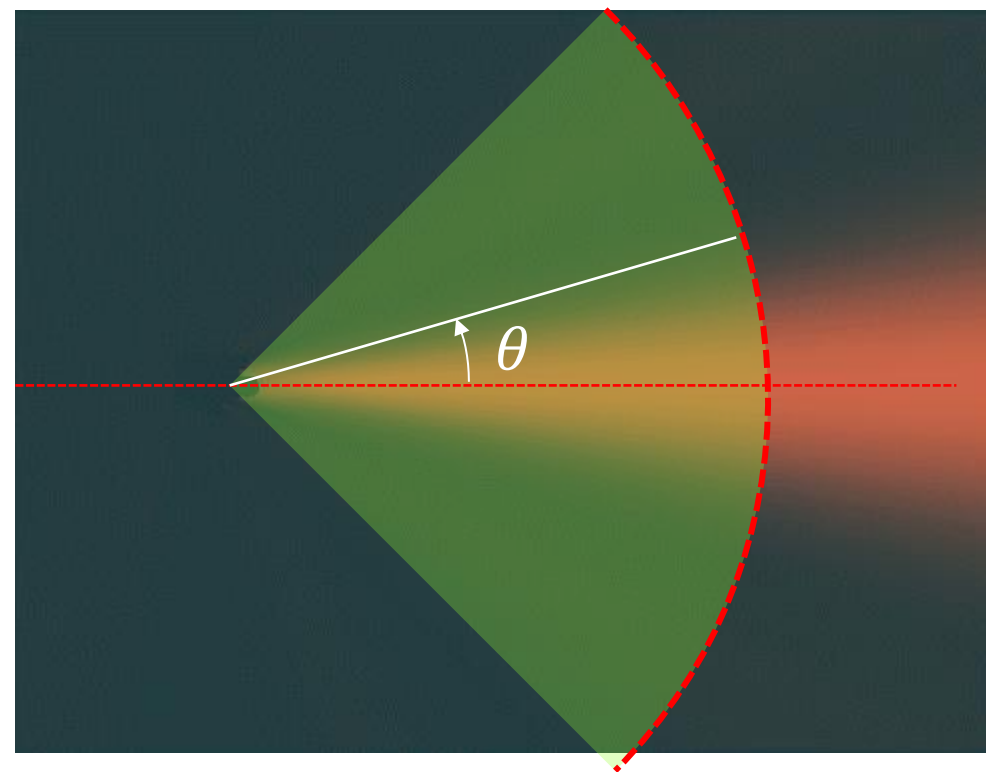
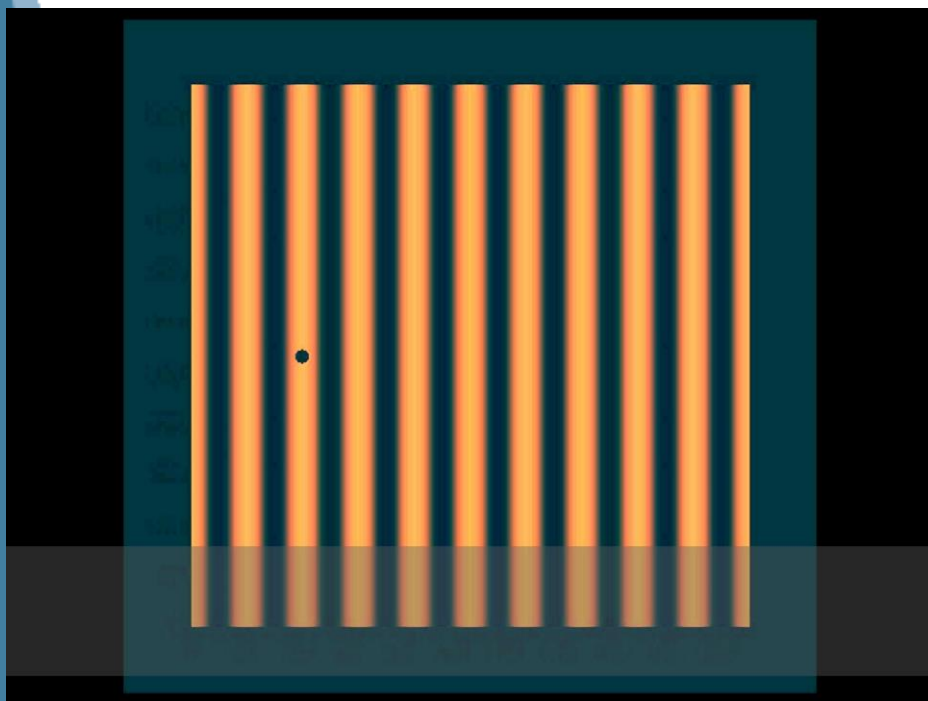
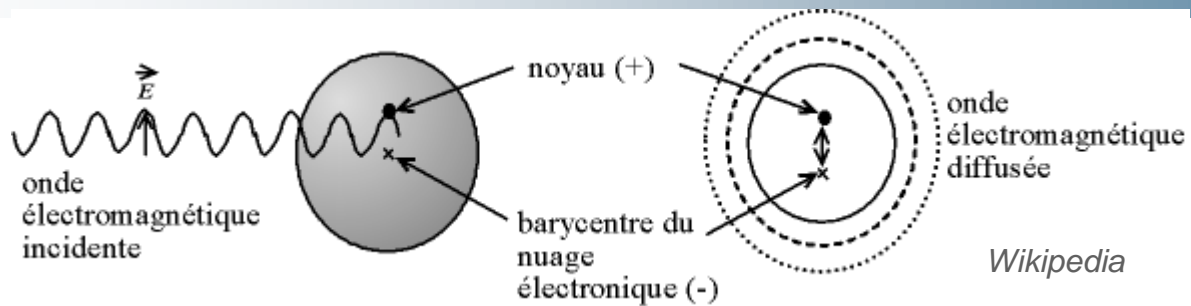
$$\vec{E} = \frac{qa}{4\pi\epsilon_0 r^3} (2\cos(\theta)\vec{u}_r + \sin(\theta)\vec{u}_\theta)$$

Thus, in the scattering plane ($\theta = \frac{\pi}{2}$):

$$\vec{E} = \frac{qa}{4\pi\epsilon_0 r^3} \vec{u}_\theta$$

The scattered electric field is isotropically distributed. The scattered electric field has the same frequency (elastic interaction).

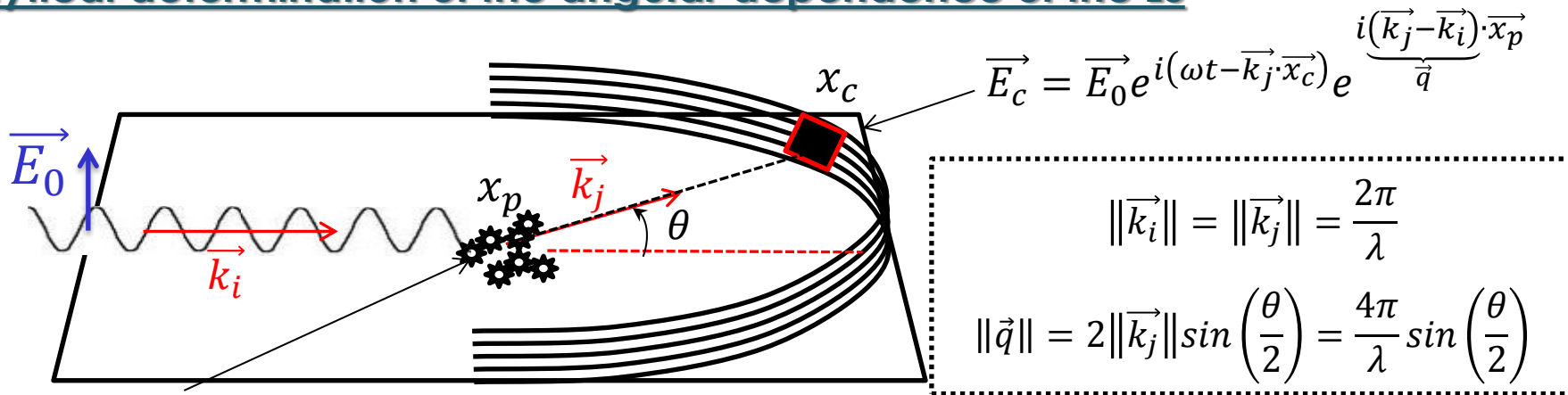
In-situ measurements : Angular Light Scattering



The dipolar approach permits to understand the link between particle size and the scattered pattern.

In-situ measurements : Angular Light Scattering

Analytical determination of the angular dependence of the LS



$$\vec{E}_c = \vec{E}_0 e^{i(\omega t - \vec{k}_i \cdot \vec{x}_p)}$$

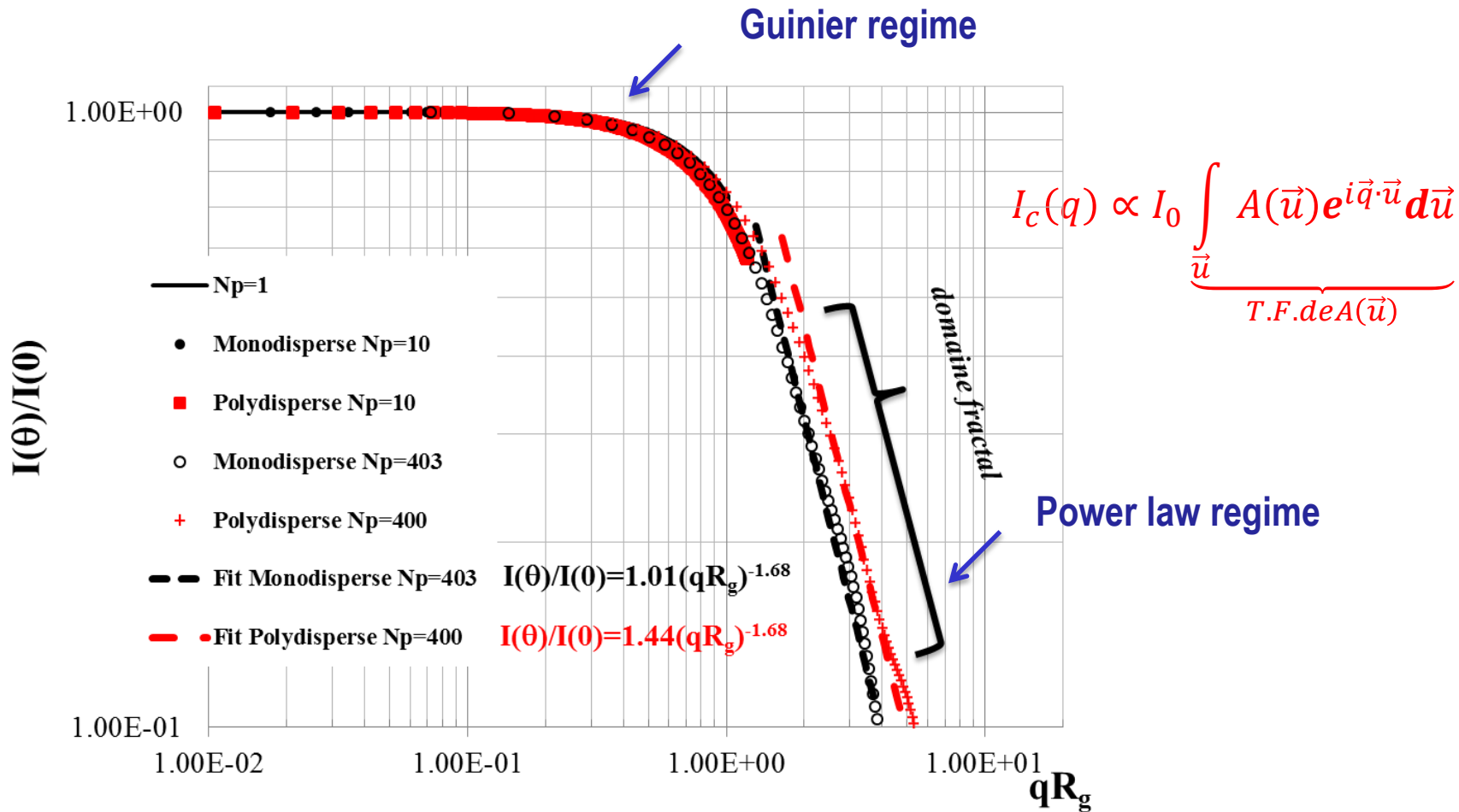
Mass spatial repartition

$$\vec{E}_c(\theta) = \vec{E}_0 e^{i(\omega t - \vec{k}_j \cdot \vec{x}_c)} \underbrace{\int_{\vec{x}_p} n(\vec{x}_p) e^{i\vec{q} \cdot \vec{x}_p} d\vec{x}_p}_{T.F. de n}$$

$$I_c(\theta) \propto \vec{E}_c(\theta) * \vec{E}_c^*(\theta) = I_0 \left(\int_{\vec{x}_p} n(\vec{x}_p) e^{i\vec{q} \cdot \vec{x}_p} d\vec{x}_p \right)^2 \propto I_0 \underbrace{\int_{\vec{u}} A(\vec{u}) e^{i\vec{q} \cdot \vec{u}} d\vec{u}}_{T.F. de A(\vec{u})}$$

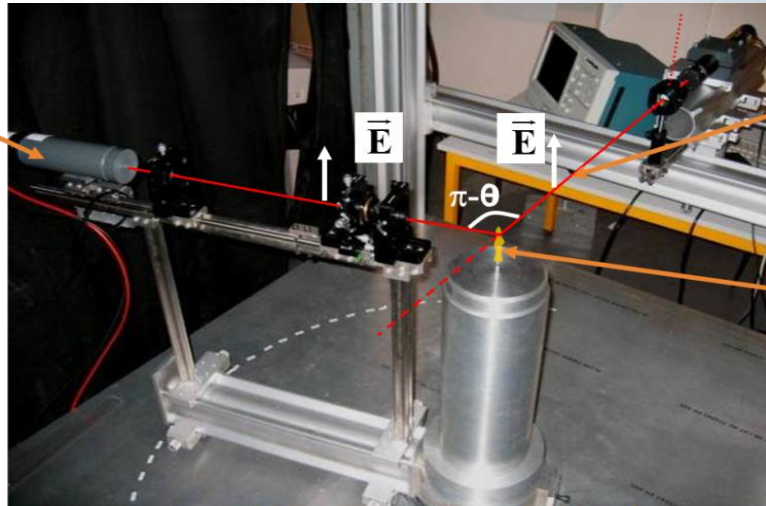
$$\text{with } A(\vec{u}) = \iiint n(\vec{r}) n(\vec{r} - \vec{u}) d\vec{r}$$

In-situ measurements : Angular Light Scattering



$$q = \frac{4\pi}{\lambda} \sin\left(\frac{\theta}{2}\right)$$

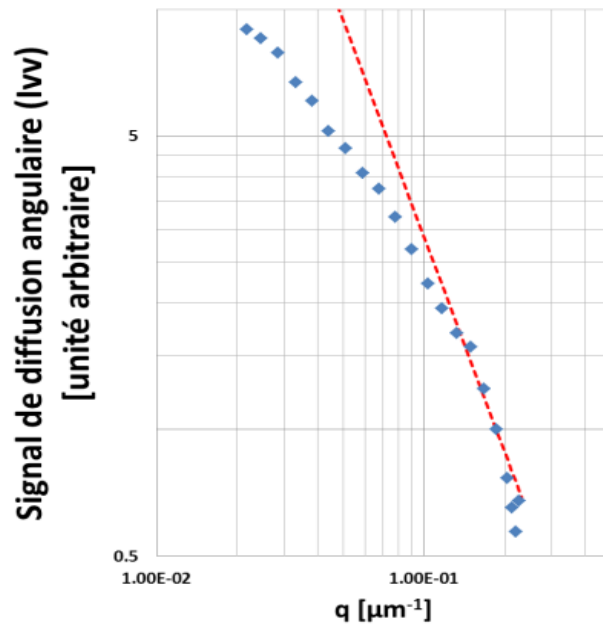
In-situ measurements : Angular Light Scattering



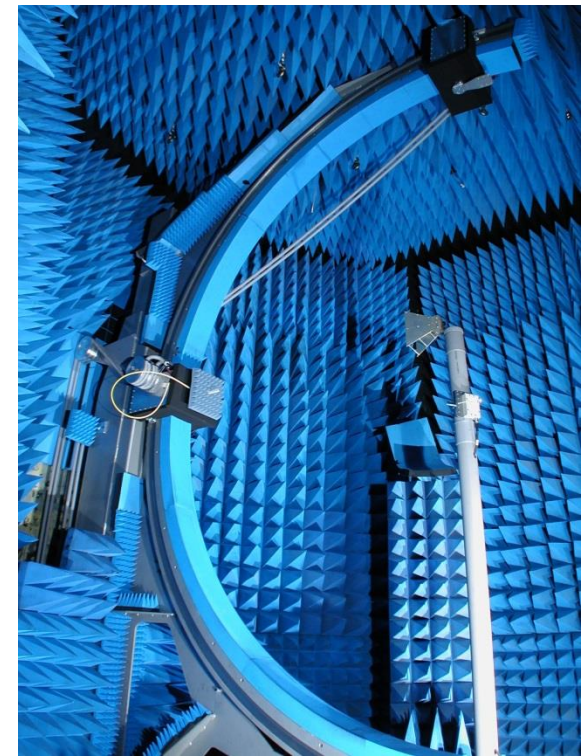
Photographie de l'installation expérimentale CORIA, juin 2007

Faisceau incident

Particules



$$q = \frac{4\pi}{\lambda} \sin\left(\frac{\theta}{2}\right)$$



Anechoic chamber at the Fresnel Institute at Marseille.

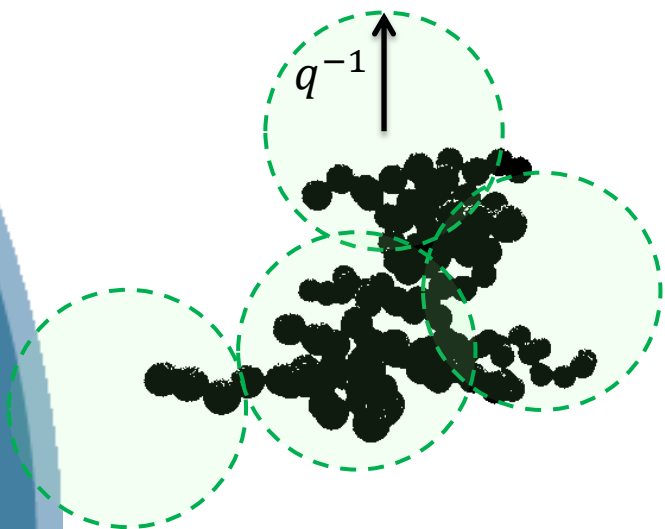
In-situ measurements : Angular Light Scattering

Analytical determination based on the q region scaling approach*

Norm of the scattering vector $\longrightarrow q = \frac{4\pi}{\lambda} \sin\left(\frac{\theta}{2}\right)$

Scattering angle \longleftarrow

\longleftarrow wavelength



$$I(q) \propto n_q N_q^2$$

q^{-1} is representative of a sphere's radius where the scattered add randomly.

n_q is the number of q-regions for a complete recovering of the aggregate

N_q is the number of scatterers in the q-region

$I(q) \propto n_q N_q^2$ By integrating the fractal properties \longrightarrow RDG – FA

*C. Sorensen, "Light scattering by fractal aggregates: a review", *Aerosol Sci. Tech.*, 35, pp. 648-687, (2001).

In-situ measurements : Angular Light Scattering

Rayleigh Debye-Gans Theory for Fractal Aggregates

$$\frac{dC_{vv}^a}{d\Omega} = N_p^2 \frac{x_p^6}{k^2} F(m) f \quad \text{et} \quad \frac{dC_{hh}^a}{d\Omega} = N_p^2 \frac{x_p^6}{k^2} F(m) f \cos(\theta)$$

$$\text{avec } x_p = \frac{\pi D_p}{\lambda}, \quad k = \frac{2\pi}{\lambda} \quad \text{et} \quad F(m) = \left| \frac{m^2 - 1}{m^2 + 2} \right|^2$$

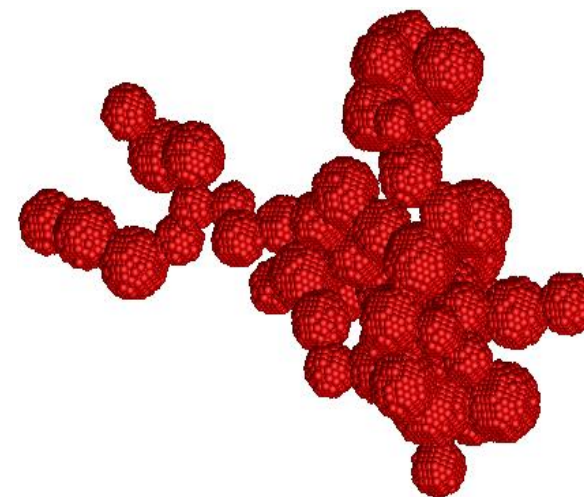
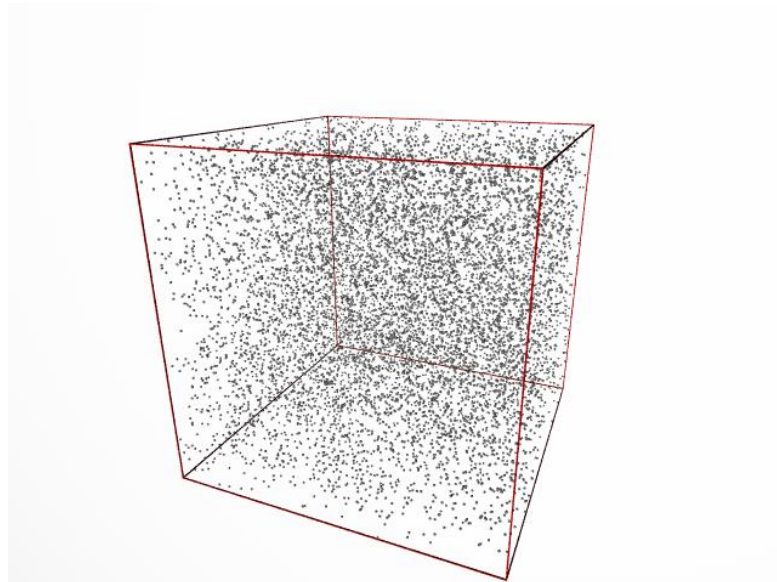
$$f(qR_g, D_f) = \exp\left(-\frac{1}{3}(qR_g)^2\right) \quad \text{si } (qR_g)^2 < \frac{3D_f}{2} \quad \text{(Guinier regime)}$$

$$f(qR_g, D_f) = \left(\frac{3D_f}{2e} \frac{1}{(qR_g)^2}\right)^{\frac{D_f}{2}} \quad \text{si } (qR_g)^2 \geq \frac{3D_f}{2} \quad \text{(Power law regime)}$$

In-situ measurements : Angular Light Scattering

Numerical / Rigorous determination of the scattering cross sections

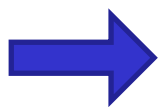
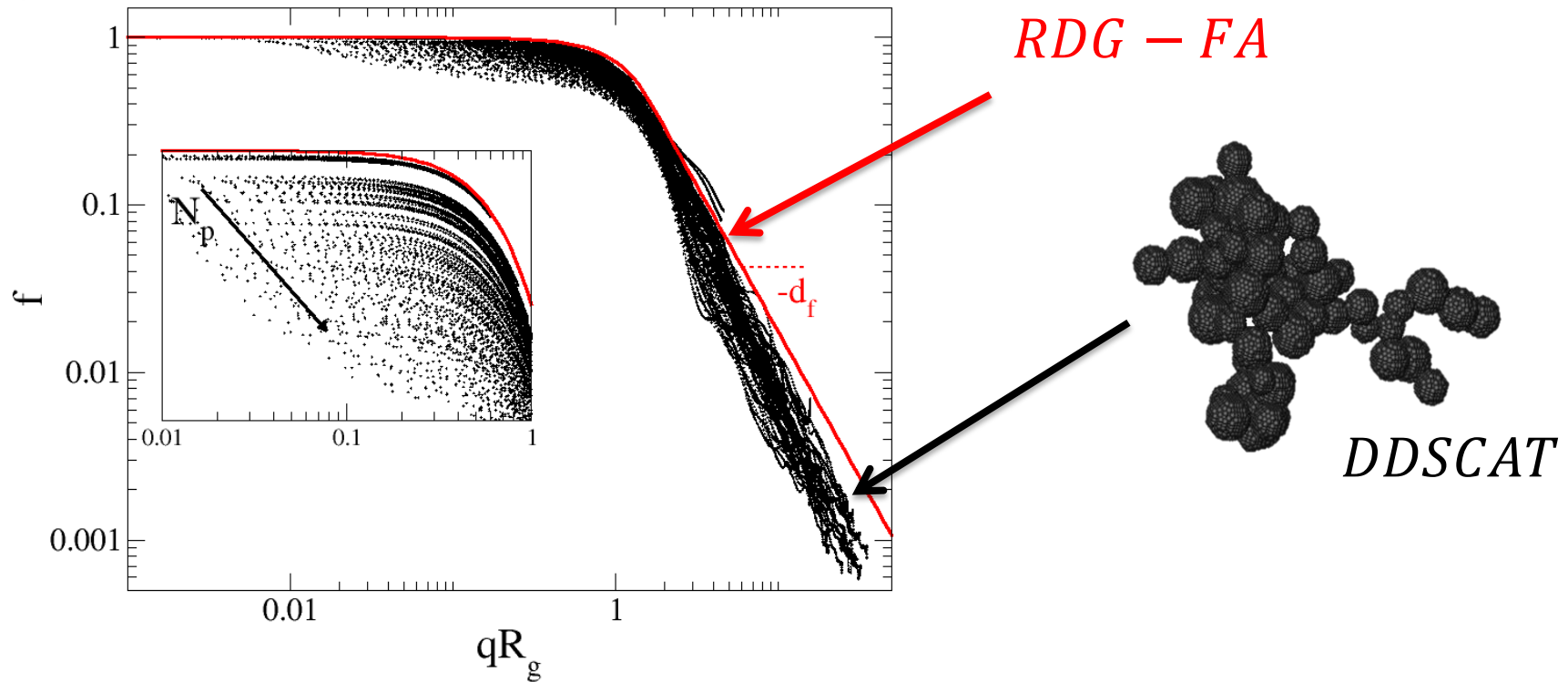
- T-Matrix (limited to simple geometries) (Mackowski / Mishchenko)
- Discret Dipole Approximation (Draine et Flatau)



Numerical virtual generation of aggregates (DLCA) and dipolar discretization for DDA calculations

In-situ measurements : Angular Light Scattering

Comparison RDG-FA - DDA



Rigorous calculations (DDSCAT) indicates a deviation from the RDG-FA theoretical approach

Yon, J., Liu, F., Bescond, A., Caumont-Prim, C., Rozé, C., Ouf, F.X., Coppalle, A. (2014). Effects of multiple scattering on radiative properties of soot fractal aggregates. *J. Quant. Spectrosc. Radiat. Transfer*, 133:374-381.

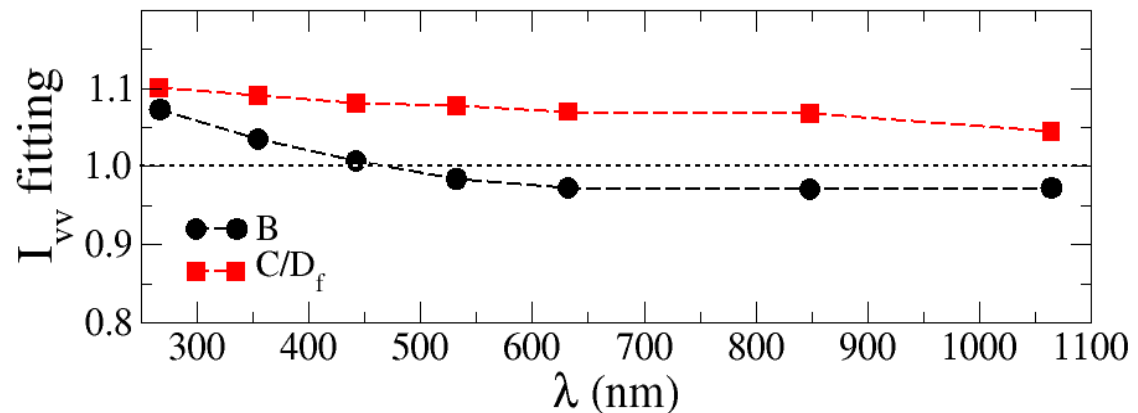
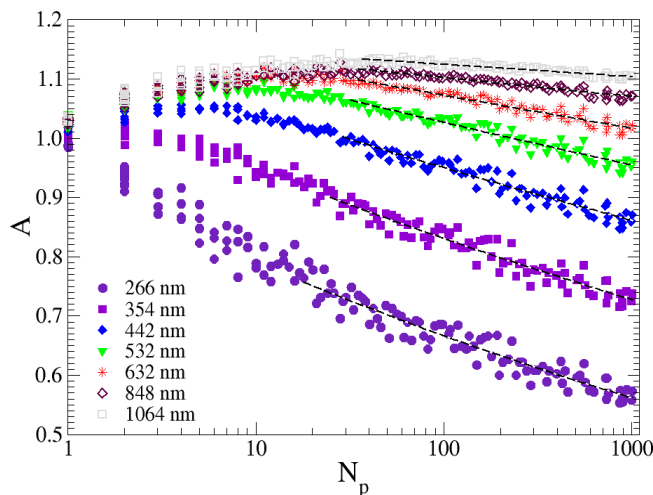
In-situ measurements : Angular Light Scattering

Determination of corrections to bring to the RDG-FA theory

$$\frac{dC_{vv}^a}{d\Omega} = N_p^2 \frac{x_p^6}{k^2} F(m) f \quad \text{with} \quad x_p = \frac{\pi D_p}{\lambda}, \quad k = \frac{2\pi}{\lambda} \quad \text{and} \quad F(m) = \left| \frac{m^2 - 1}{m^2 + 2} \right|^2$$

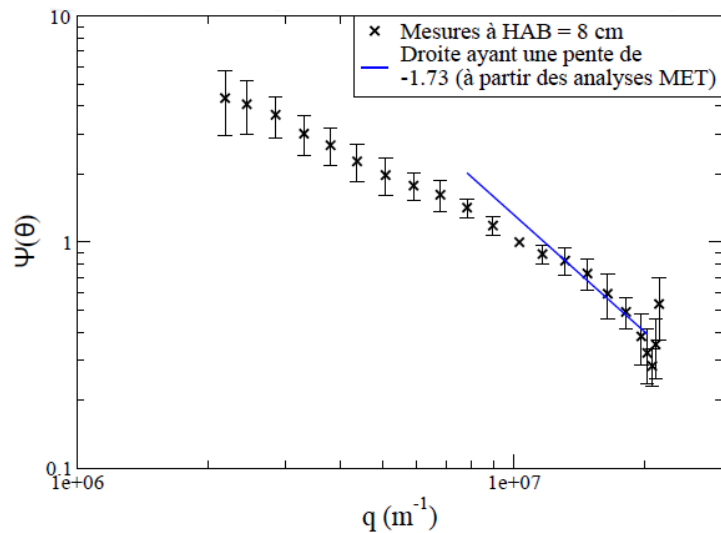
$$f(qR_g, D_f) = A \exp\left(-\frac{B}{3} (qR_g)^2\right) \quad \text{if} \quad (qR_g)^2 < \frac{3C}{2B} \quad \text{(Guinier regime)}$$

$$f(qR_g, D_f) = A \left(\frac{3C}{2Be} \frac{1}{(qR_g)^2} \right)^{\frac{C}{2}} \quad \text{if} \quad (qR_g)^2 \geq \frac{3C}{2B} \quad \text{(Power Law regime)}$$

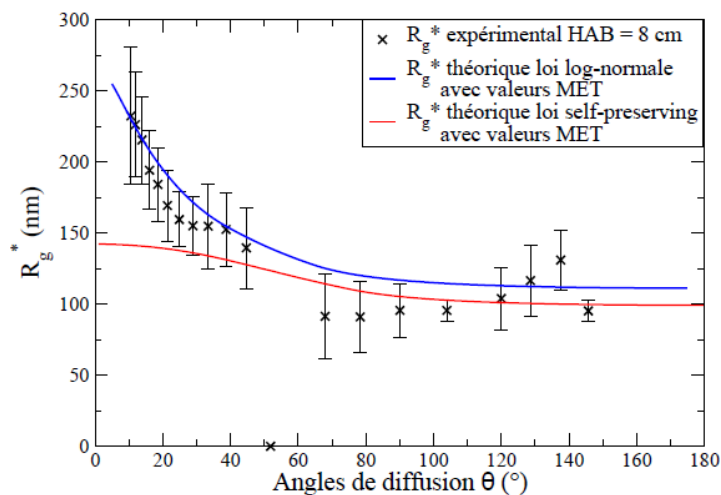


In-situ measurements : Angular Light Scattering

Application to the determination of the soot size distribution

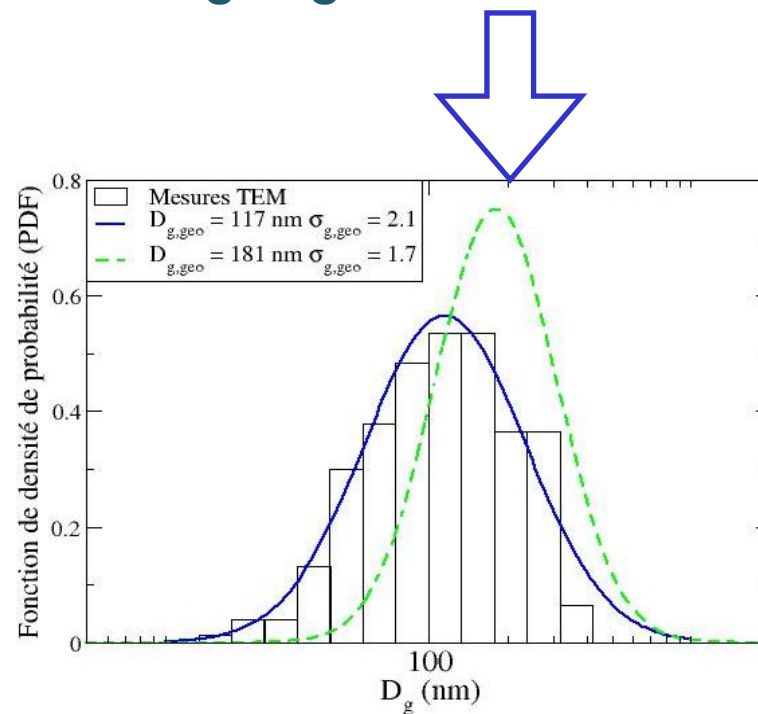


(a) Intensité diffusée normalisée $\Psi(\theta)$



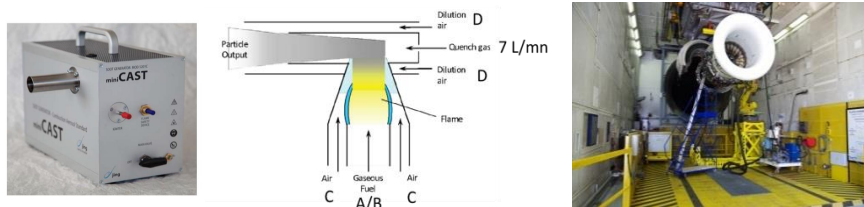
(b) Fonction $R_g^*(\theta)$

Demonstration of the ability to determine the size distribution with a measurement limited at least to 3 scattering angles.



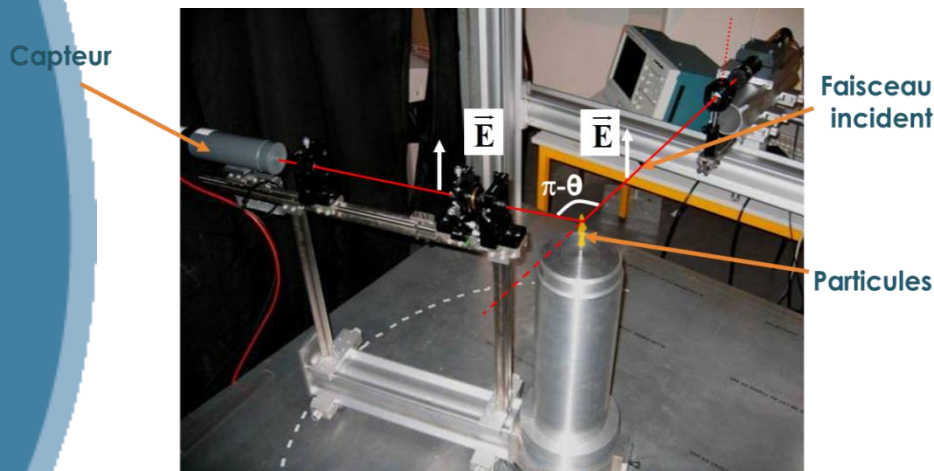
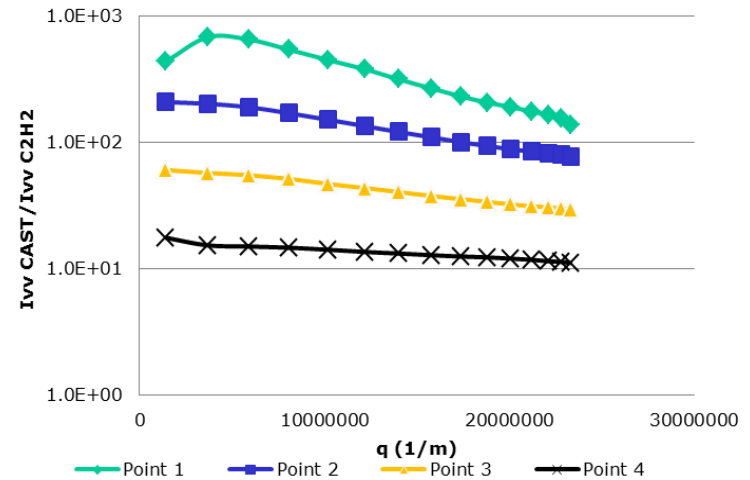
Caumont et al. *Journal of Quantitative Spectroscopy & Radiative Transfer* 126 (2013) 140–149

In-situ measurements : Angular Light Scattering

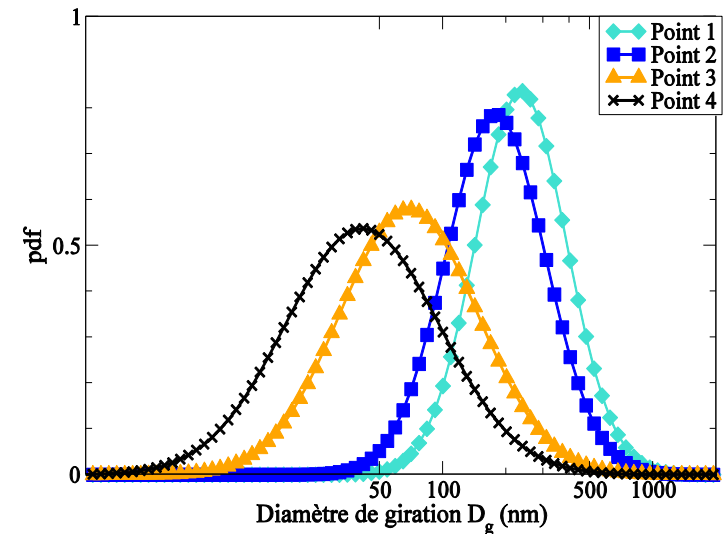


Point de fonctionnement	Débit de propane (ml/min)	Débit d'azote (ml/min)	Débit d'air d'oxydation (l/min)	Débit d'air de dilution (l/min)	OC /TC (%)
1	60	0	1.50	20	16,2
2	60	0	1.15	20	58,3
3	60	0	1.00	20	87,0
4	50	200	1,20	20	4,1

Tableau 1 : Présentation des points de fonctionnement sélectionnés du CAST



Angular light scattering bench (CORIA)

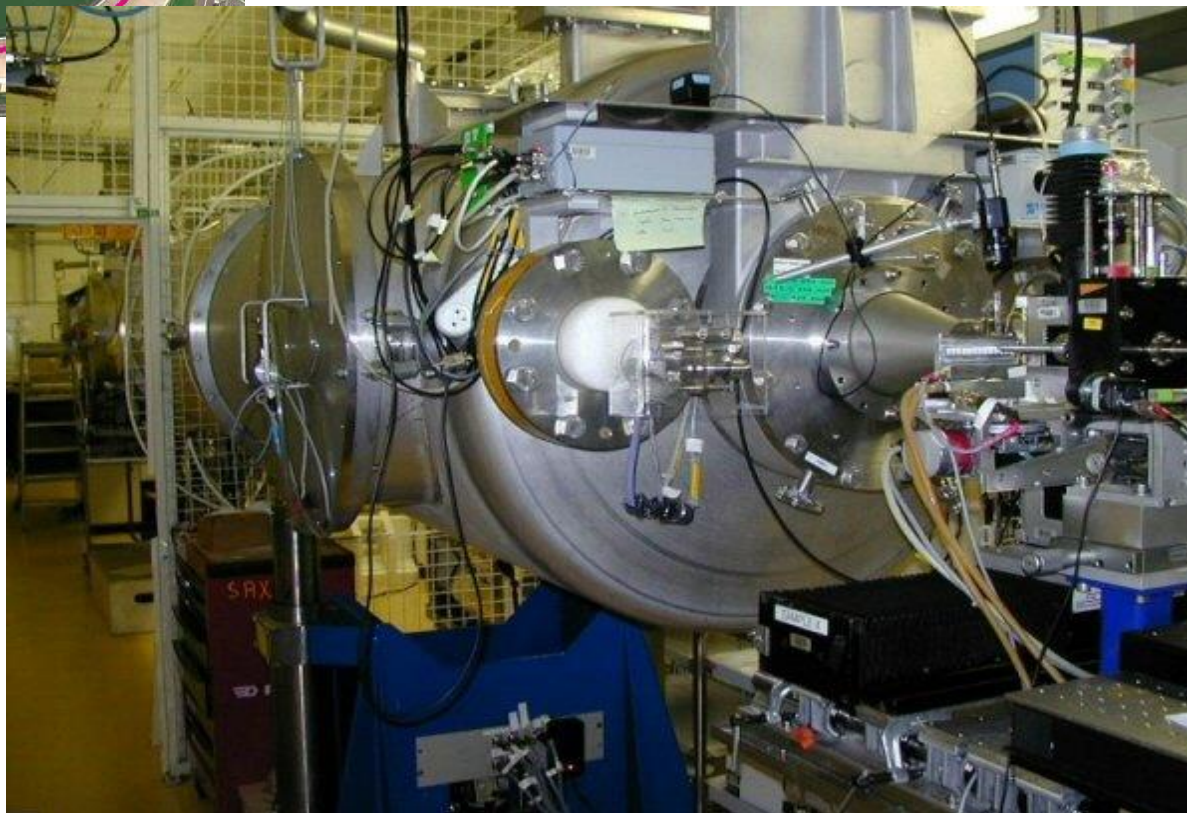


Caumont et al. *Journal of Quantitative Spectroscopy & Radiative Transfer* 126 (2013) 140–149

In-situ measurements : Small Angle X ray Scattering



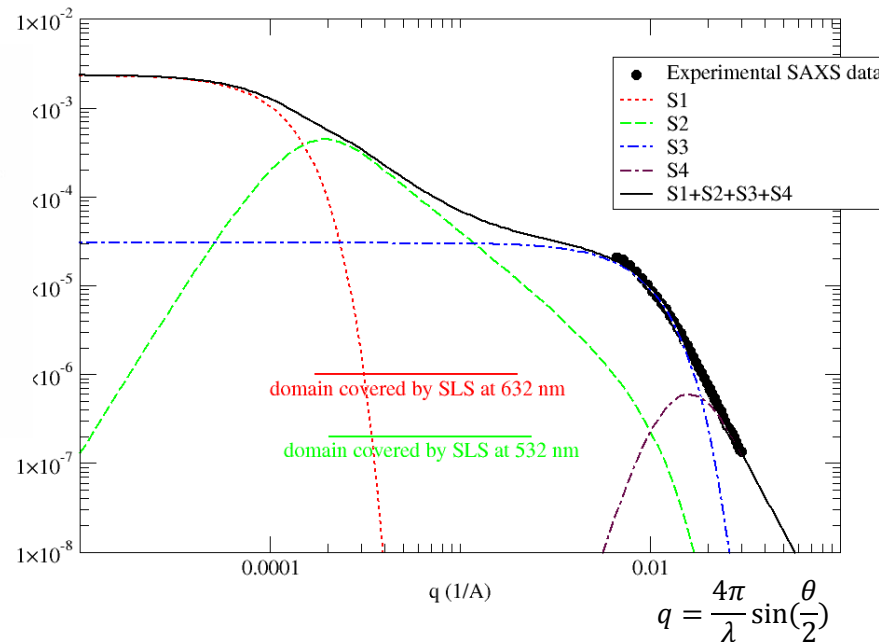
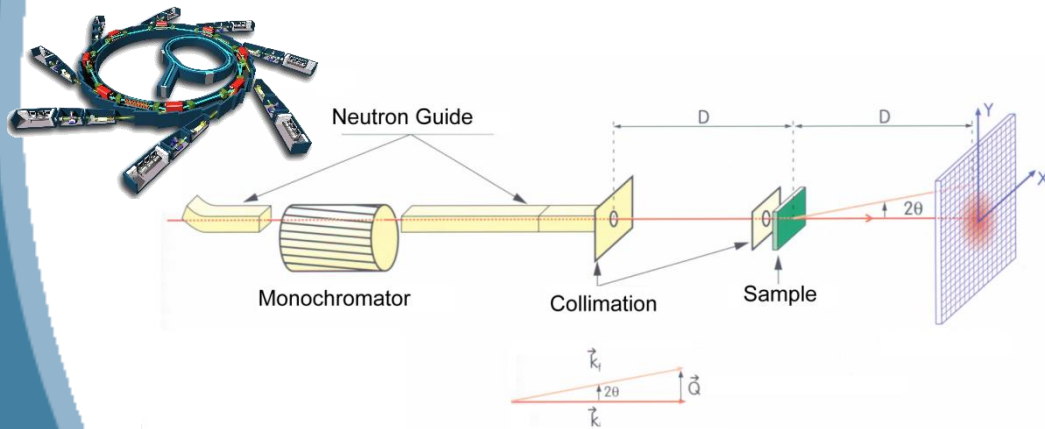
European Synchrotron Radiation Facility (Grenoble)



$$q = \frac{4\pi}{\lambda} \sin\left(\frac{\theta}{2}\right)$$

$\theta < 2^\circ$
 $\lambda \sim 10 \text{ \AA}$ (rayons X)

In-situ measurements : Small Angle X ray Scattering



Beaucage model for two scales components
 (aggregats & primary spheres, Beaucage, G.
 Journal of Applied Crystallography 1995, 28, 717-728.):

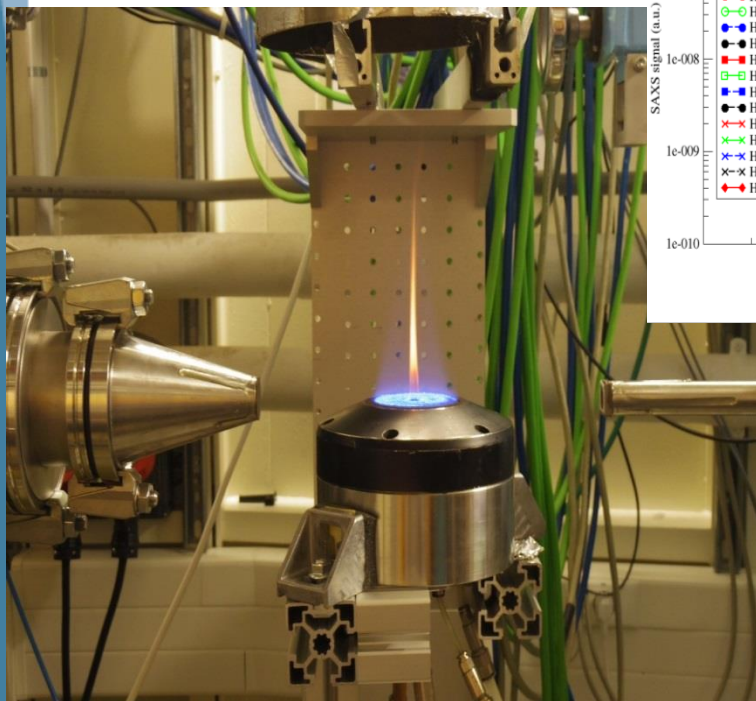
$$S = \underbrace{G_a \exp\left(-\frac{q^2 R_{ga}^2}{3}\right)}_{S1} + \underbrace{\frac{1.62 G_a \cdot PDI_a}{R_{ga}^4} \left(\frac{\left[\text{erf}\left(\frac{q R_{ga}}{6^{0.5}}\right) \right]^{3D_f}}{q^{D_f}} \right) \exp\left(-\frac{q^2 R_{gp}^2}{3}\right)}_{S2} + \underbrace{G_p \exp\left(-\frac{q^2 R_{gp}^2}{3}\right)}_{S3} + \underbrace{\frac{1.62 G_p \cdot PDI_p}{R_{gp}^4} \left(\frac{\left[\text{erf}\left(\frac{q R_{gp}}{6^{0.5}}\right) \right]^{3p}}{q^p} \right)}_{S4}$$

4 components (more sensitive) least square fitting of the data

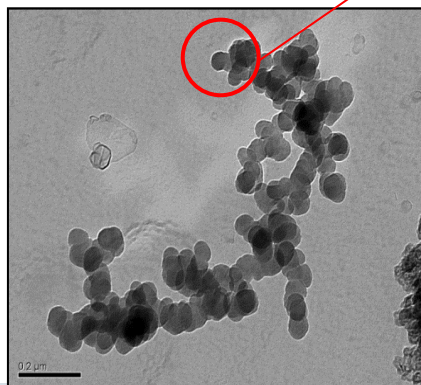
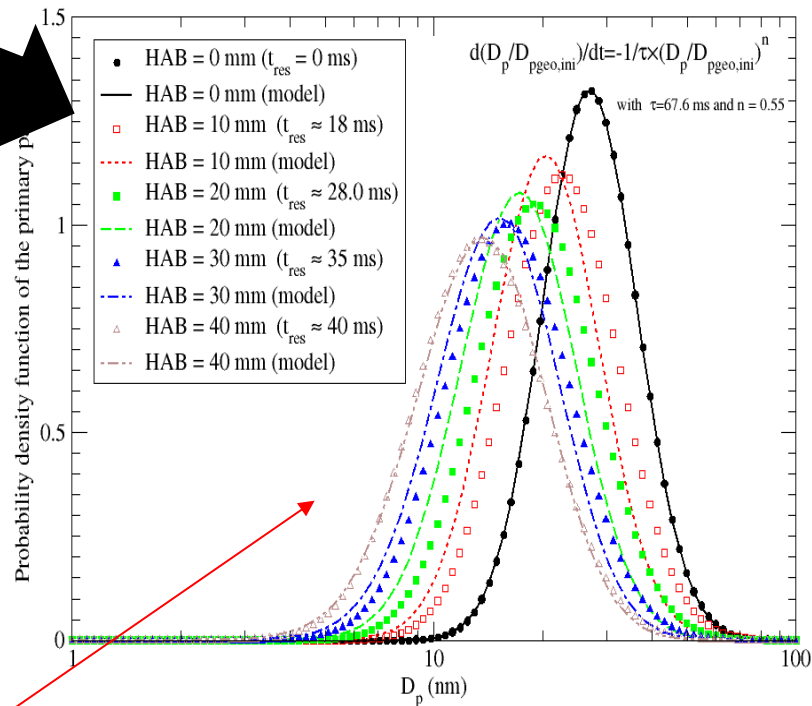
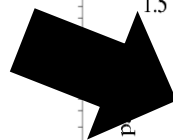
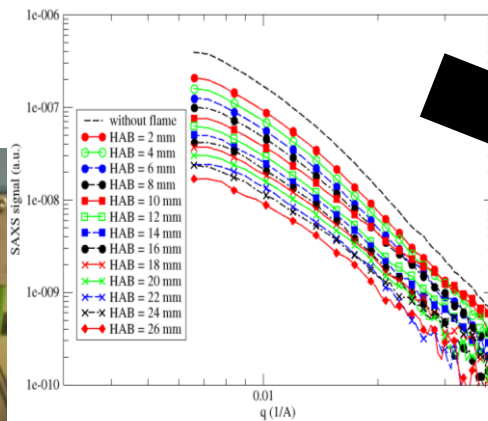


R_{gp} and PDI_p → Determination of the primary particle size distribution (assumed to be lognormal)

In-situ measurements : Small Angle X ray Scattering



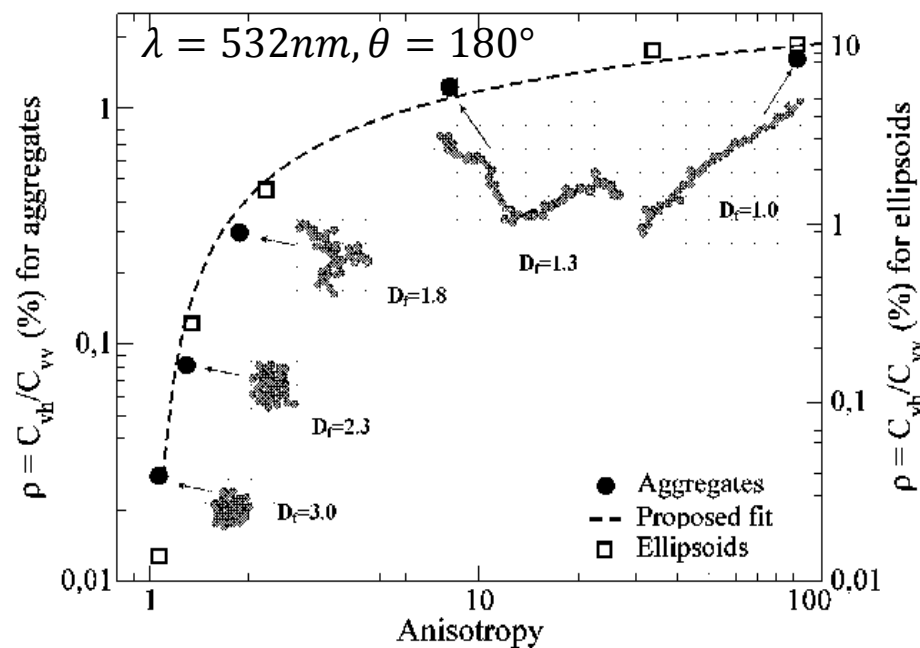
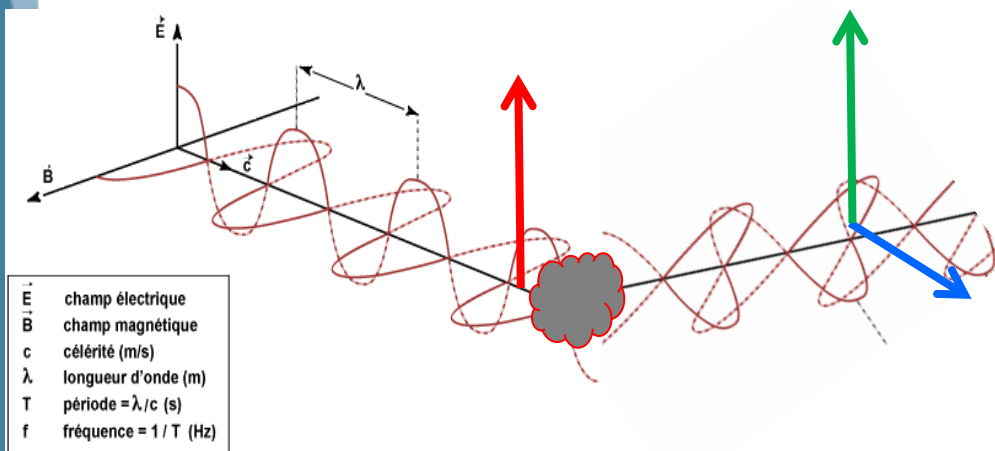
**Experiments conducted at
synchrotron SOLEIL
(June 2015)**



In-situ measurements : Depolarization ratios

RDG-FA predicts the scattering cross sections for vv and hh polarizations but considers $C_{vh} = C_{hv} = 0$.

$$\rho = \frac{C_{vh}}{C_{vv}}$$



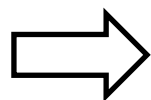
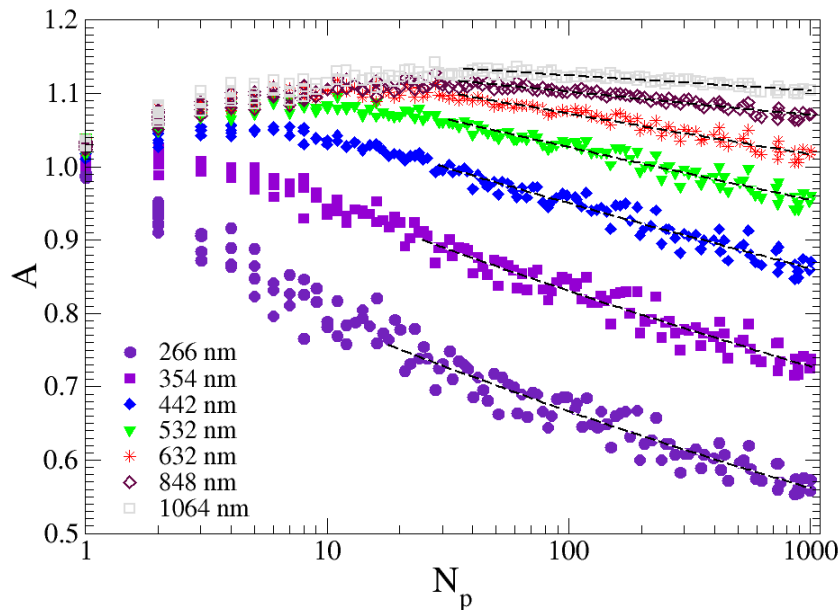
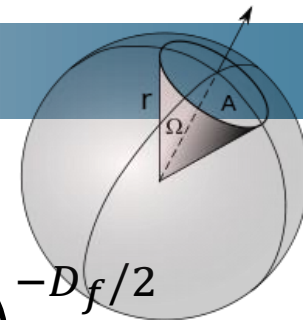
That measurement informs us of the particle shape.
This is used for LIDAR measurements.

A. Bescond et al. "Numerical investigation of the possibility to determine the primary particle size of fractal aggregates by measuring light depolarization", *J. Quant. Spectrosc. Radiat. Transfer*, 126, pp. 130-139, (2013).

In-situ measurements : total light scattering cross section

RDG-FA for total scattering

$$C_d^a = [A] N_p^2 \frac{8\pi x_p^6}{3k^2} F(m) g \quad \text{avec} \quad g = \left(1 + \frac{4}{3D_f} (kR_g)^2 \right)^{-D_f/2}$$



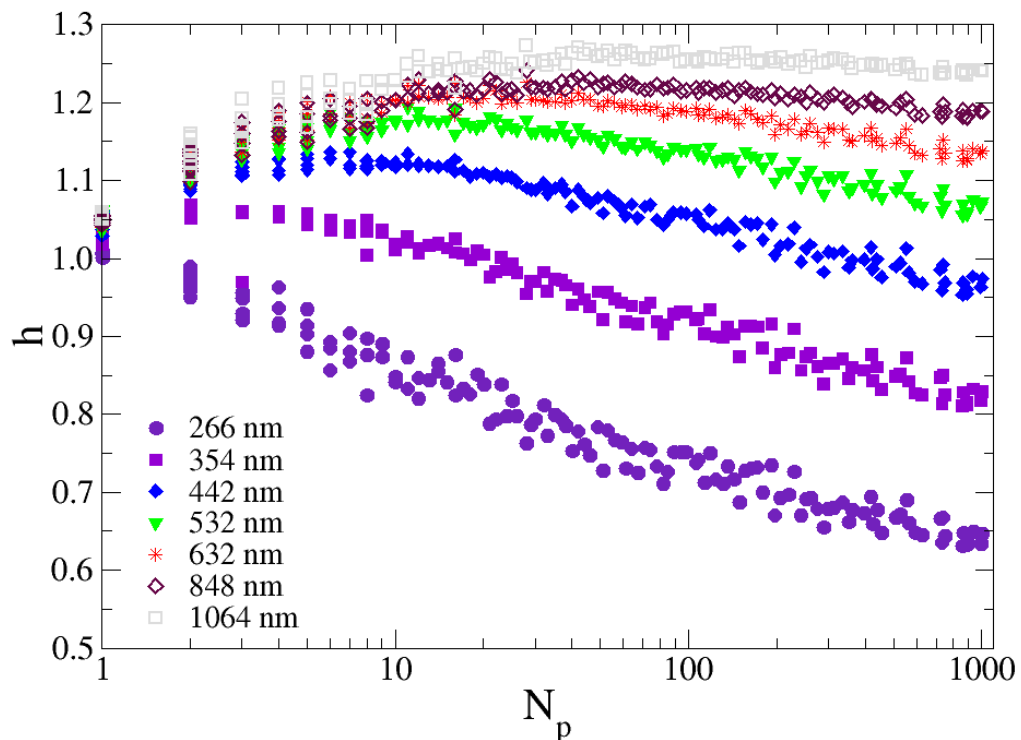
SLS is heighten by MS at large λ
and reduced at small λ (shielding effects)

with $x_p = \frac{\pi D_p}{\lambda}$, $k = \frac{2\pi}{\lambda}$ and $F(m) = \left| \frac{m^2 - 1}{m^2 + 2} \right|^2$

In-situ measurements : Absorption cross section

RDG-FA for absorption

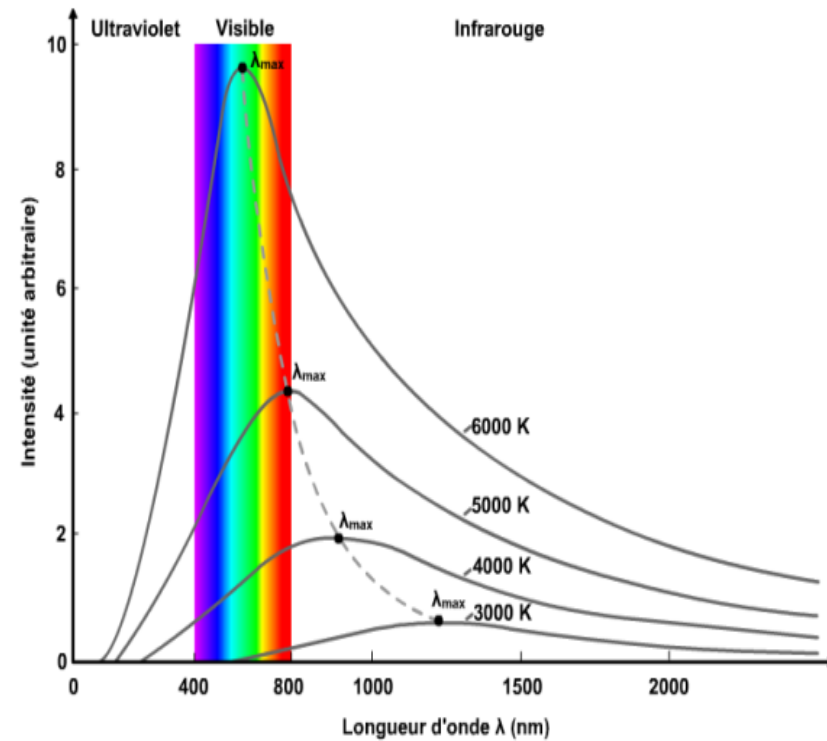
$$C_{abs}^a = [h] N_p \frac{4\pi x_p^3}{k^2} E(m) \text{ with } E(m) = \text{Im} \left(\frac{m^2 - 1}{m^2 + 2} \right)$$



$$\text{with } x_p = \frac{\pi D_p}{\lambda}, k = \frac{2\pi}{\lambda}$$

In-situ measurements : Laser Induced Incandescence

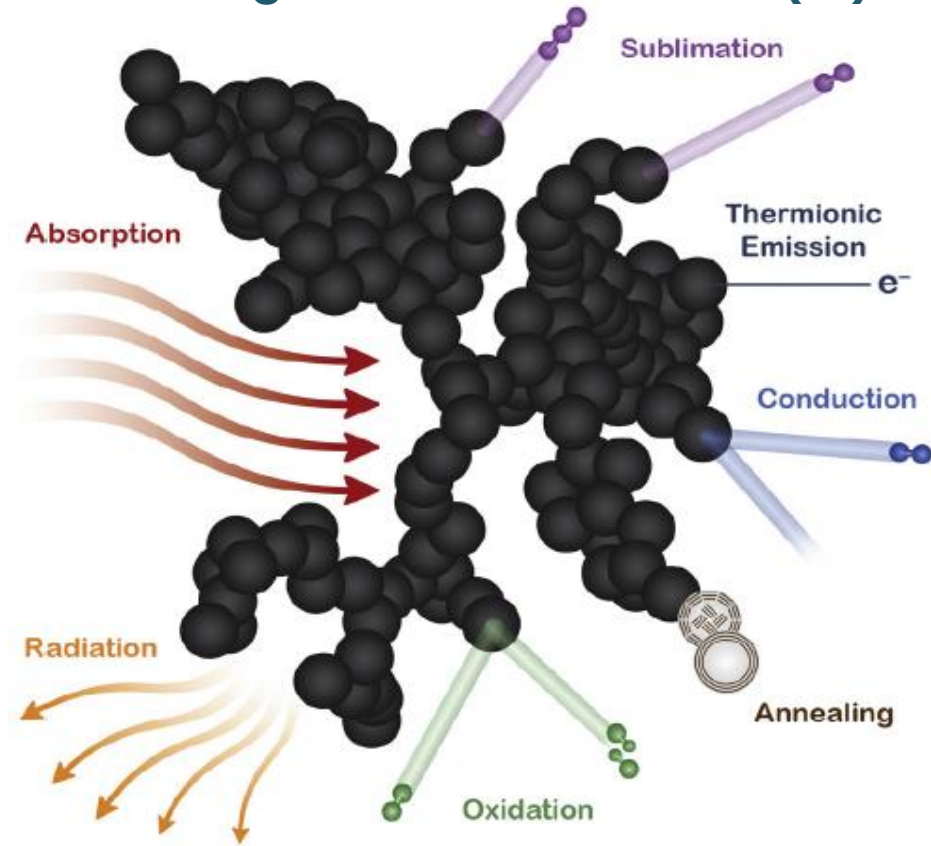
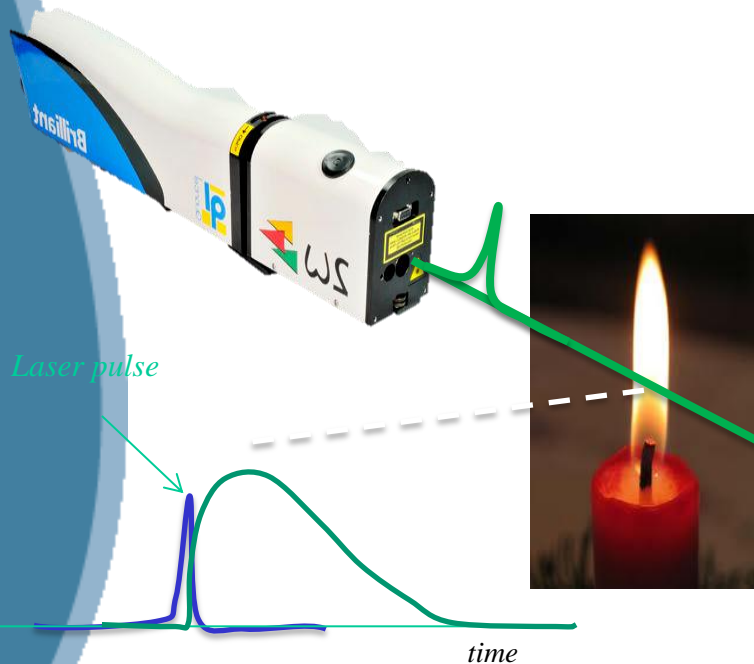
At high temperatures, absorbing particles can have a spectral radiance predicted by the black body Plank's law.



<http://hebergement.u-sud.fr/projetsdephysiquestatistique/>

In-situ measurements : Laser Induced Incandescence

The soot temperature can be increased by irradiating the particles with an intense laser pulse and the incandescence signal can be collected (LII).



H. A. Michelsen, C. Schulz, G. J. Smallwood, and S. Will, "Laser-induced incandescence: Particulate diagnostics for combustion, atmospheric, and industrial applications," Progress in Energy and Combustion Science.

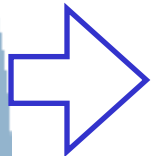
In-situ measurements : Laser Induced Incandescence

Conclusion, Soot optical index, Coupling, LII, ρ , SAXS, SLS, ρ_{eff} SMPS, d_p intro

$$LII(\lambda_{det}) = \varepsilon_{\lambda_{det}} \frac{\eta_{\lambda_{det}}}{D^2} L_{\lambda_{det},T}^{\circ} \Delta S d\lambda_{det}$$



$$\varepsilon_{\lambda} = K_{abs}(\lambda) \Delta x$$



$$LII(\lambda_{det}) = \frac{\Delta V C_1 \eta_{\lambda_{det}}}{D^2} K_{abs}(\lambda_{det}) \frac{1}{\lambda_{det}^5} \left(\exp\left(\frac{C_2}{\lambda_{det} T}\right) - 1 \right)^{-1} \Delta \lambda_{det}$$



RDG-FA


$$K_{abs}(\lambda) = N_{tot} \int_0^{\infty} C_{abs}^{mono}(\lambda) N_p p(N_p) dN_p$$

In-situ measurements : Laser Induced Incandescence

$$LII(\lambda_{det}) = \frac{\pi^2 \Delta V C_1 \eta \lambda_{det}}{D^2} D_p^3 N_{tot} \underbrace{\int_0^\infty N_p p(N_p) dN_p}_{\overline{N_p}} \frac{E(m, \lambda_{det})}{\lambda_{det}^6} \left(\exp\left(\frac{C_2}{\lambda_{det} T}\right) - 1 \right)^{-1} \Delta \lambda_{det}$$

Or,

$$f_v = \frac{\pi D_p^3}{6} N_{tot} \underbrace{\int_0^\infty N_p p(N_p) dN_p}_{\overline{N_p}}$$

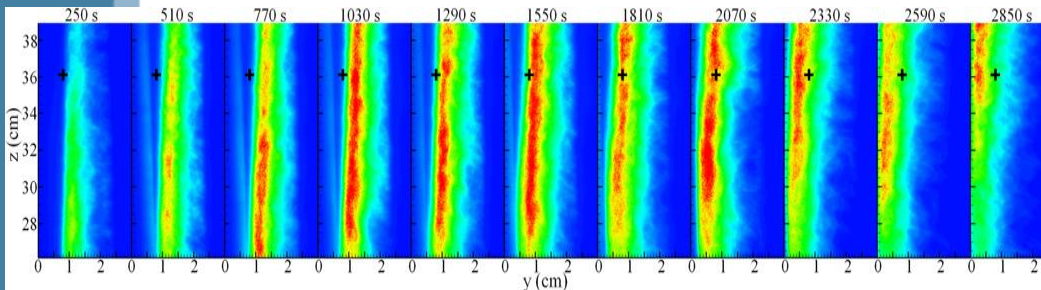
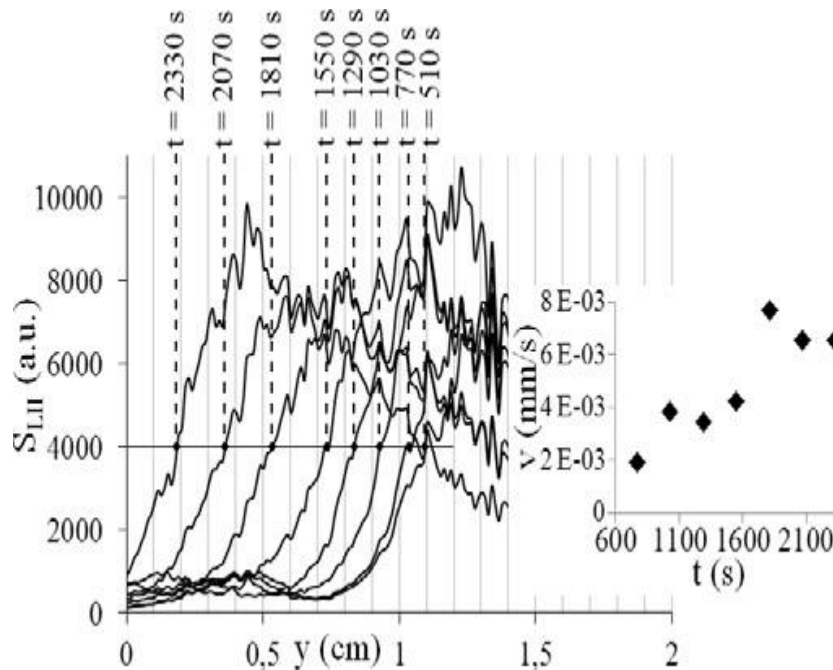
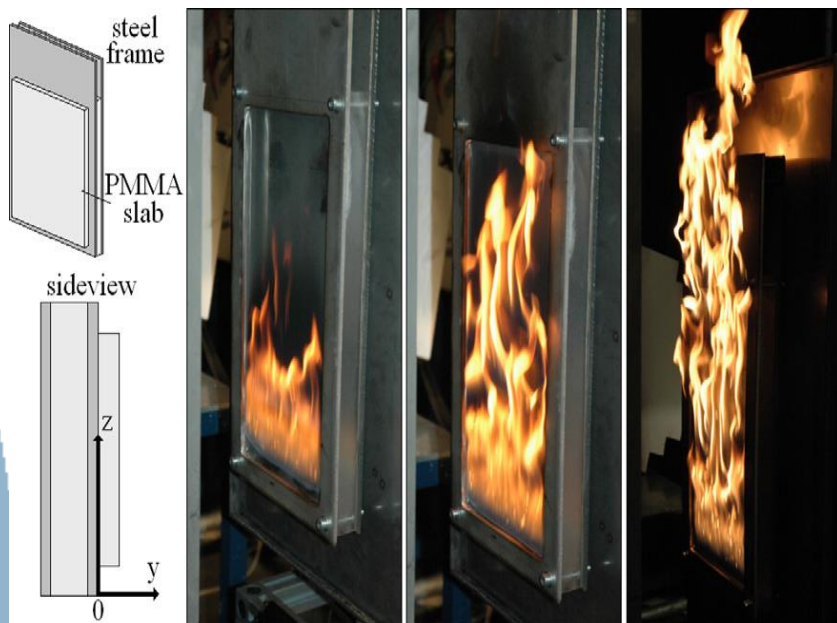


$$LII = \frac{6\pi^2 \Delta V C_1 \eta \lambda_{det}}{D^2} f_v \frac{E(m, \lambda_{det})}{\lambda_{det}^6} \left(\exp\left(\frac{C_2}{\lambda_{det} T}\right) - 1 \right)^{-1} \Delta \lambda_{det}$$

That technique enables the determination of in-situ planar cartographies of the soot volume fractions

In-situ measurements : Laser Induced Incandescence

Control of solid combustible material pyrolysis by LII

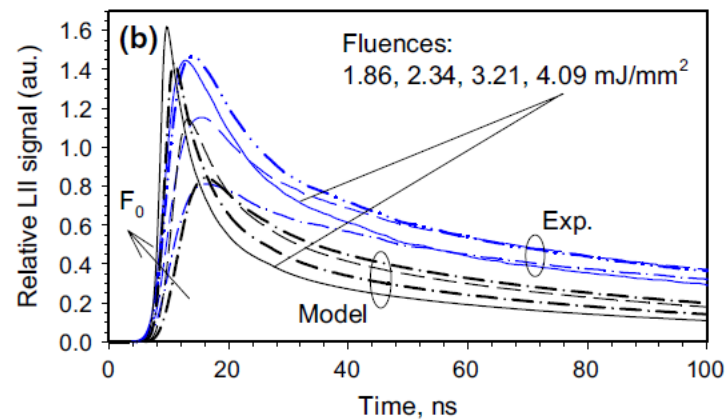
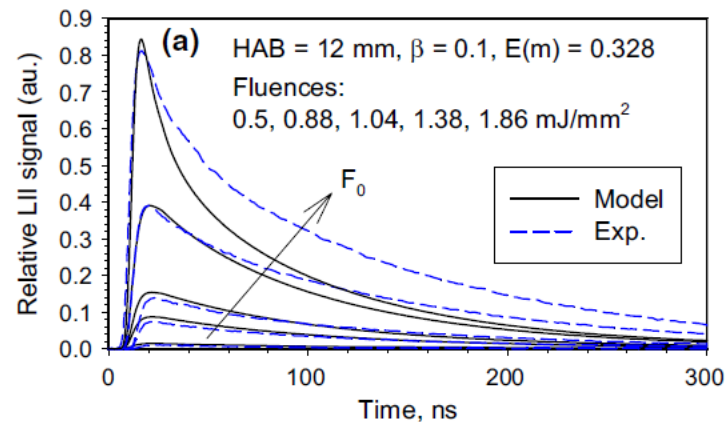


D. Hebert, A. Coppalle, and M. Talbaut, "2D soot concentration and burning rate of a vertical PMMA slab using Laser-Induced Incandescence," *Proceedings of the Combustion Institute*, 2012.

In-situ measurements : Laser Induced Incandescence

$$\underbrace{\rho C_p \frac{\pi}{6} D_p^3(t) \frac{dT}{dt}}_{\text{heating}} = \underbrace{\frac{\pi^2 D_p^3 E(m)}{\lambda_{laser}}}_{\text{absorption}} F(t) - \underbrace{\frac{2 K_a \pi D_p^2}{D_p(t) + G l_{pm}}}_{\text{conduction}} (T - T_0) - \underbrace{\frac{199 \pi^3 D_p^3(t) k_b^5 E(m)}{h(hc)^3}}_{\text{Radiation}} (T^5 - T_0^5) + \underbrace{\frac{\Delta H_v}{W_s} \frac{dM}{dt}}_{\text{Sublimation}}$$

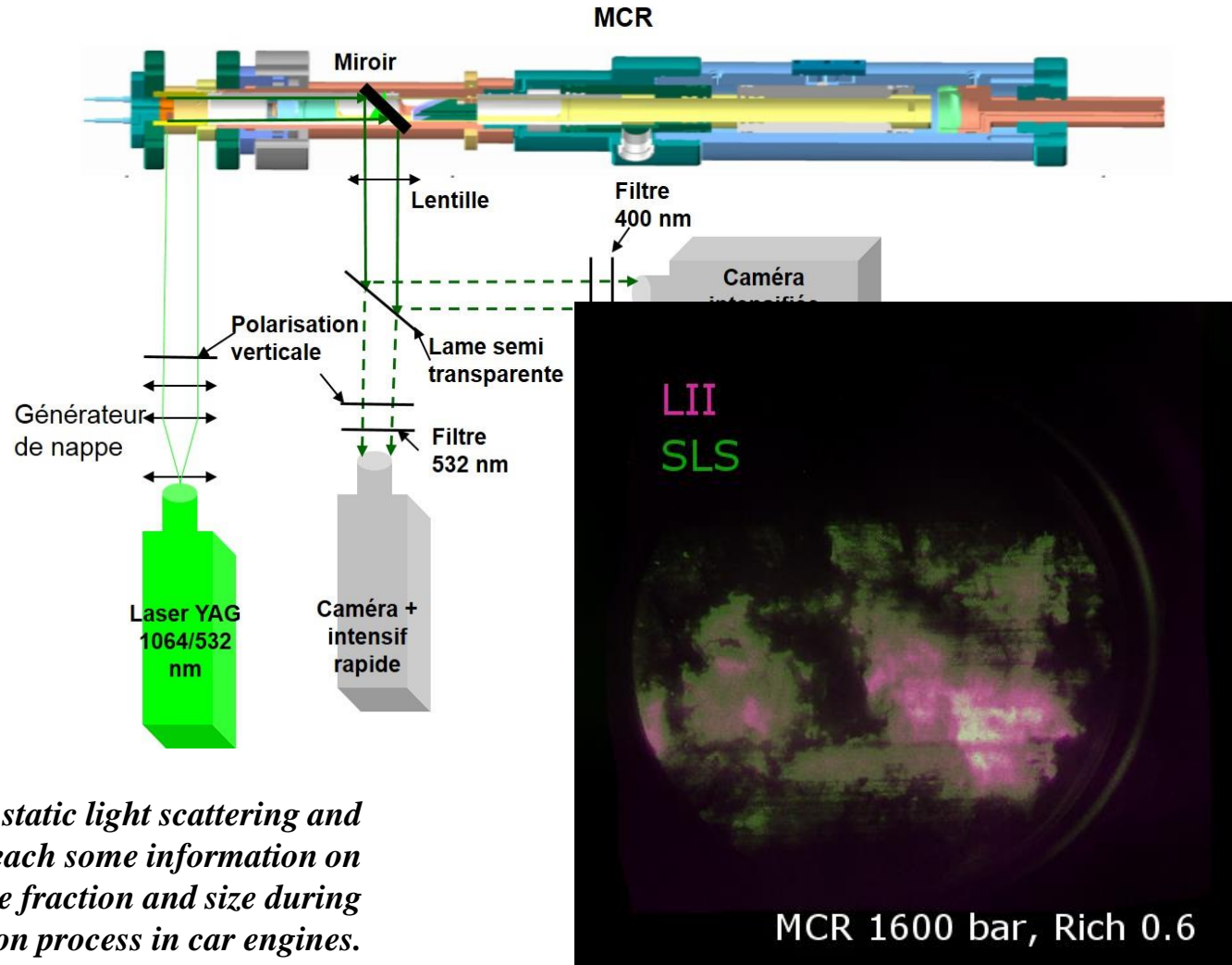
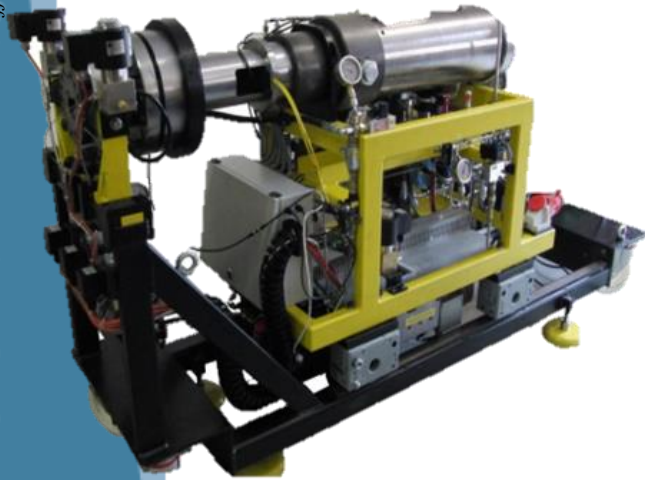
By using a LII model, the temporal decay of the LII signal can be interpreted in term of primary particle diameter (not the diameter of the aggregate!).



S. Bejaoui, S. Batut, E. Therssen, N. Lamoureux, P. Desgroux et F. Liu, "Measurements and modeling of laser-induced incandescence of soot at different heights in a flat premixed flame", *App. Phys. B-Lasers O*, 118, pp. 449-469, (2015). 10.1007/s00340-015-6014-3

In-situ measurements : Examples of couplings of different techniques

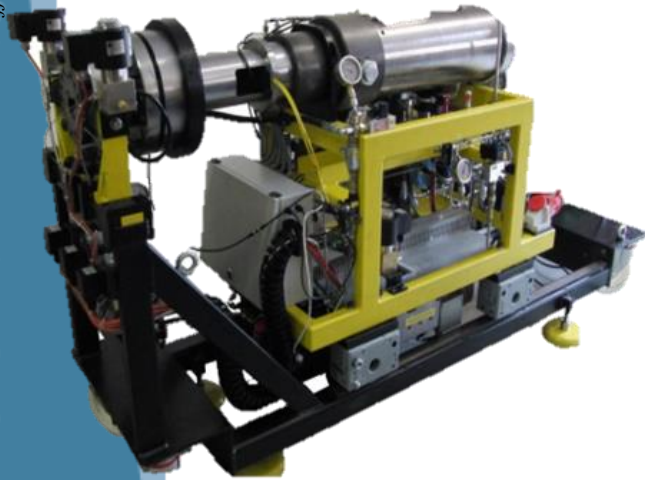
Last example of coupling for the characterization of soot in a Rapid Compression Machine.



Coupling of static light scattering and LII permits to reach some information on soot volume fraction and size during combustion process in car engines.

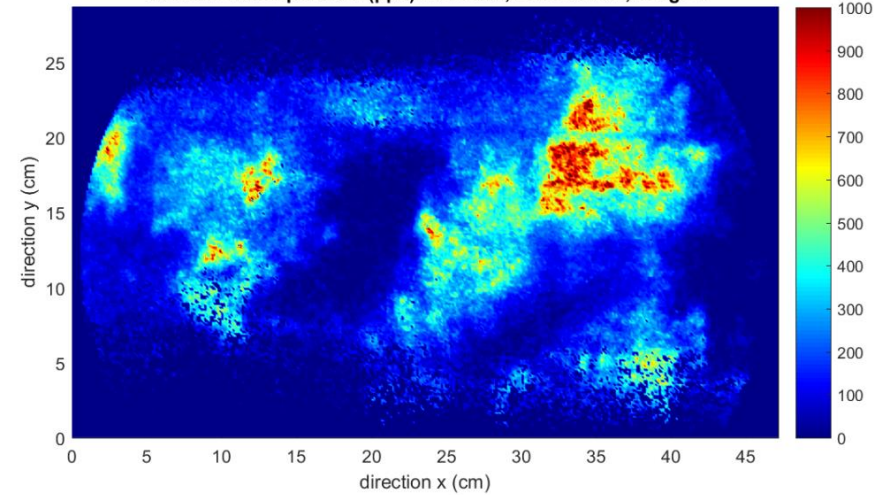
In-situ measurements : Examples of couplings of different techniques

Last example of coupling for the characterization of soot in a Rapid Compression Machine.

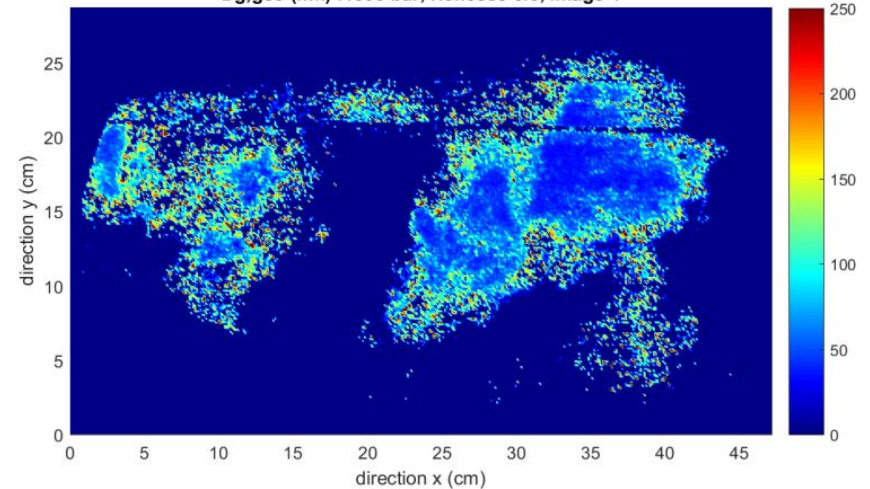


Coupling of static light scattering and LII permits to reach some information on soot volume fraction and size during combustion process in car engines.

fraction volumique MCR (ppb) :1600 bar, richesse 0.6, image 4



Dg,geo (nm) :1600 bar, richesse 0.6, image 4



Soot optical index

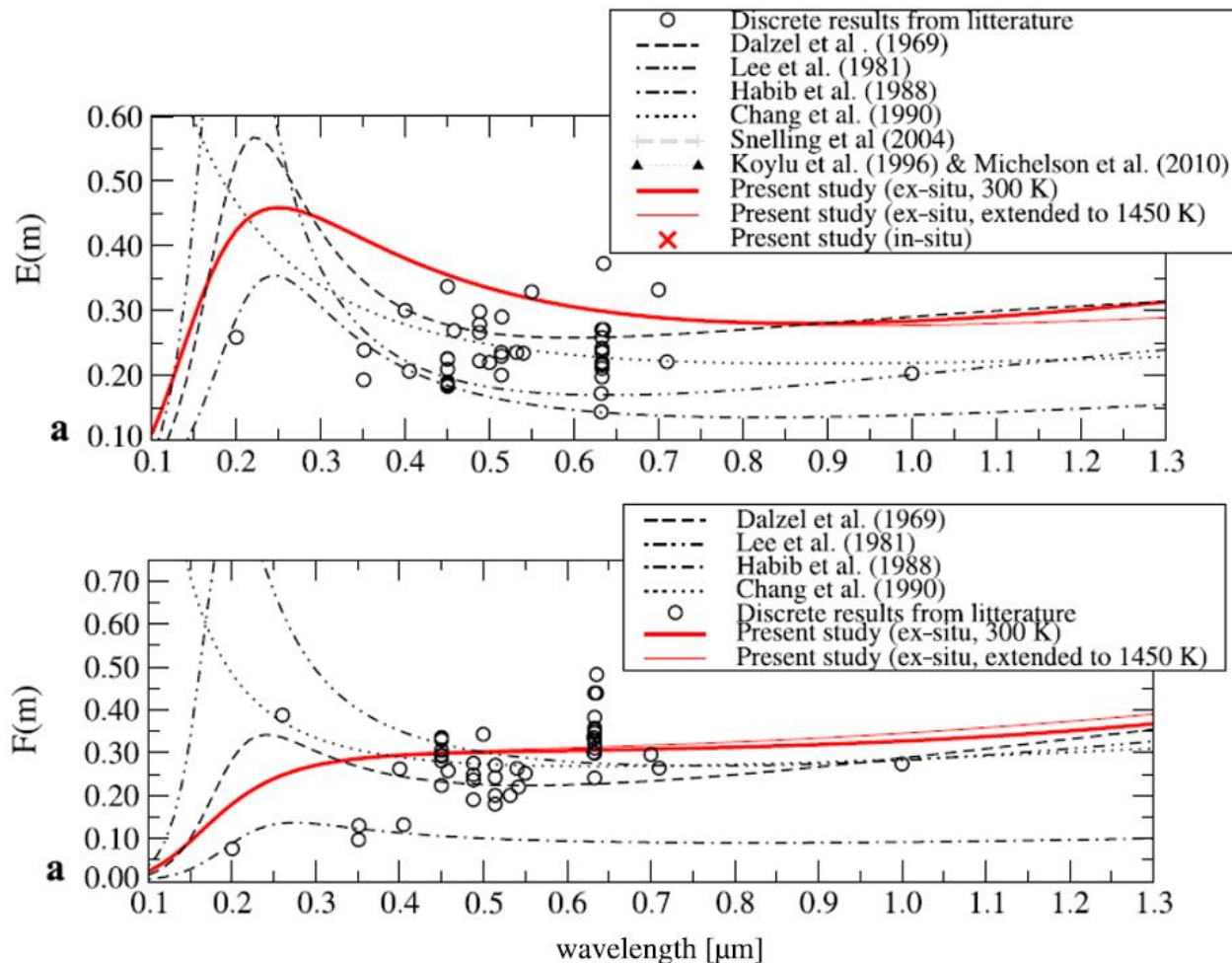
For a quantitative use of optical diagnostics and for the evaluation of soot radiative transfer (engines, glass industry, visibility during fires, global warming), optical index is a key parameter.



Soot is strongly absorbing, in consequence the optical index is complex $m = n + ik$. It is a macroscopic parameter related to the dielectric constant $\epsilon = m^2$. In Rayleigh theory and for many diagnostics, it is expressed through the absorption and scattering functions :

$$E(m) = \text{Im} \left(\frac{m^2 - 1}{m^2 + 2} \right), F(m) = \left| \frac{m^2 - 1}{m^2 + 2} \right|^2$$

Soot optical index

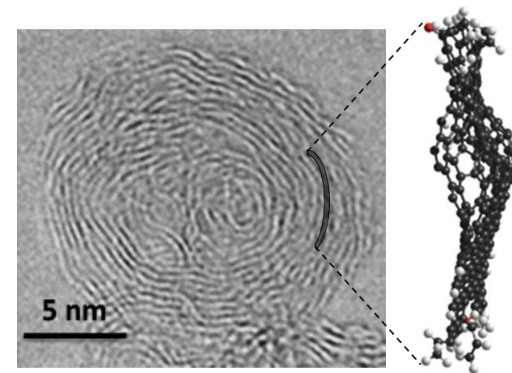
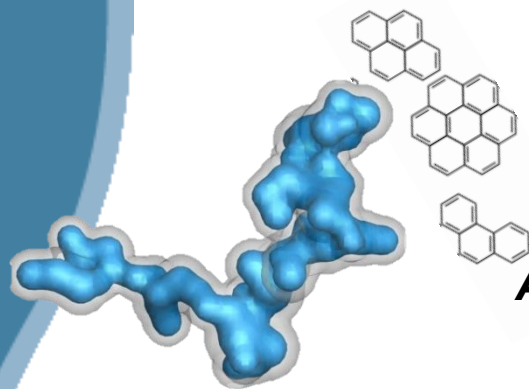


The optical indexes reported in the literature are dispersed.

Soot optical index

Soot composition and thus optical index may vary strongly according to :

- Elemental composition H/C ?
- Carbon atoms arrangement sp^3 (diamond like) / sp^2 (graphite like)
- Size of the crystallites
- Presence Organic compounds (OC/TC)



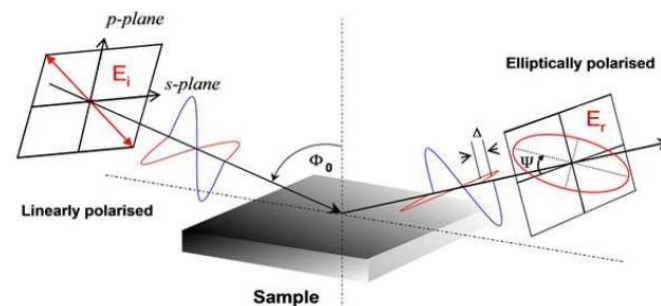
All these characteristics change with time during soot formation.

We speak about “aging process” or “soot maturity”

Soot optical index

Ellipsometry

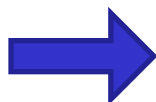
Analysis of the change of polarization state upon reflection or transmission.



Φ_0 : angle of incidence
 Δ : relative phase change
 Ψ : relative amplitude change

s-plane stands perpendicularly to the plane of incidence
 p-plane stands parallel to the plane of incidence

Need to compact soot to form a thin layer, intrusive operation ?



There is a need for an aerosol phase based method !

Soot optical index

Two Excitation Wavelength Laser Induced Incandescence method.

(PC2A / Eric Therssen's method)

The thermal emission is provoked by the absorption of nanosecond laser pulses.

By considering the Rayleigh absorption cross section by the primary spheres :

$$C_{abs} = \frac{8\pi^2 a^3}{\lambda} E(m) \text{ with } E(m) = -I_m \left\{ \frac{m^2 - 1}{m^2 + 2} \right\}$$

The more E(m) is, the more the radiation is intense.

TEW-LII method consists in adapting the laser fluence on different particles or with different wavelengths in order to reach the same thermal emission.

The ratio of the laser energies is directly related to the ratio of E(m) functions.



It is an in-situ method but a relative determination of E(m).

Optical index is only partially determined.

S. Bejaoui, R. Lemaire, P. Desgroux et E. Therssen, "Experimental study of the $E(m, \lambda)/E(m, 1064)$ ratio as a function of wavelength, fuel type, height above the burner and temperature", **Appl. Phys. B-Lasers O**, 116, pp. 313-323, (2014). [10.1007/s00340-013-5692-y](https://doi.org/10.1007/s00340-013-5692-y)

Soot optical index

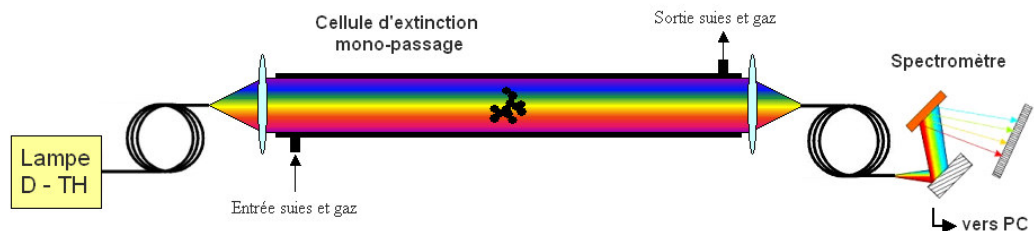
Extinction Spectra Analysis.

(current method)

Transmitted light with and without soot particles is spectrally recorded.

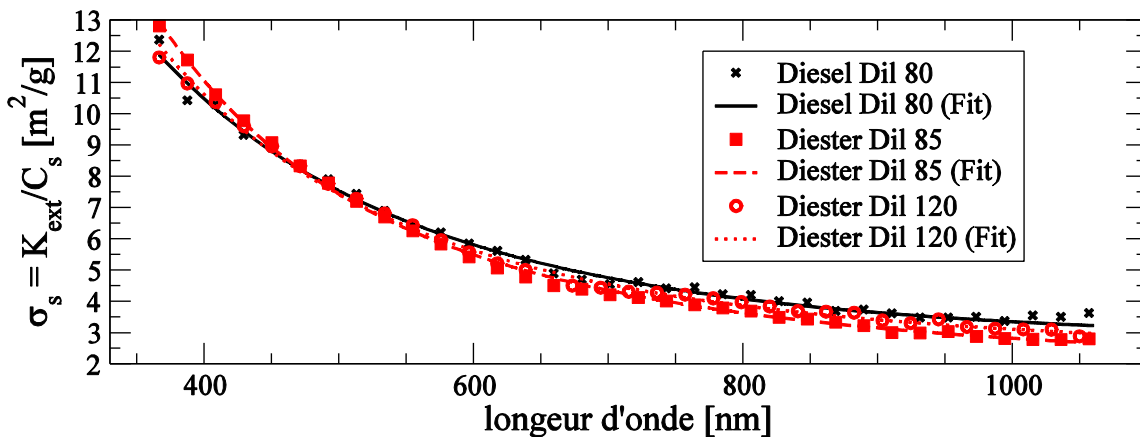
Extinction coefficient is easily determined by applying the Bouguer-Lambert's law :

$$K_{ext} = -\frac{1}{L} \ln \left(\frac{I}{I_0} \right) \text{ with } K_{ext} = (C_{abs} + C_{scat})N$$



That extinction spectra is then normalized by the soot mass concentration to provide the **mass specific extinction** (m^2/g).

$$\sigma_s = K_{ext} / C_s$$



Soot optical index

Inversion procedure based on RDG-FA theory and Lorentz-Drude model

The corrected version of the RDG-FA theory permits to reach a simple analytical expression of the extinction cross sections whose precision is quite identical to their rigorous determination with intensive solving of the Maxwell equation.

The specific extinction becomes :

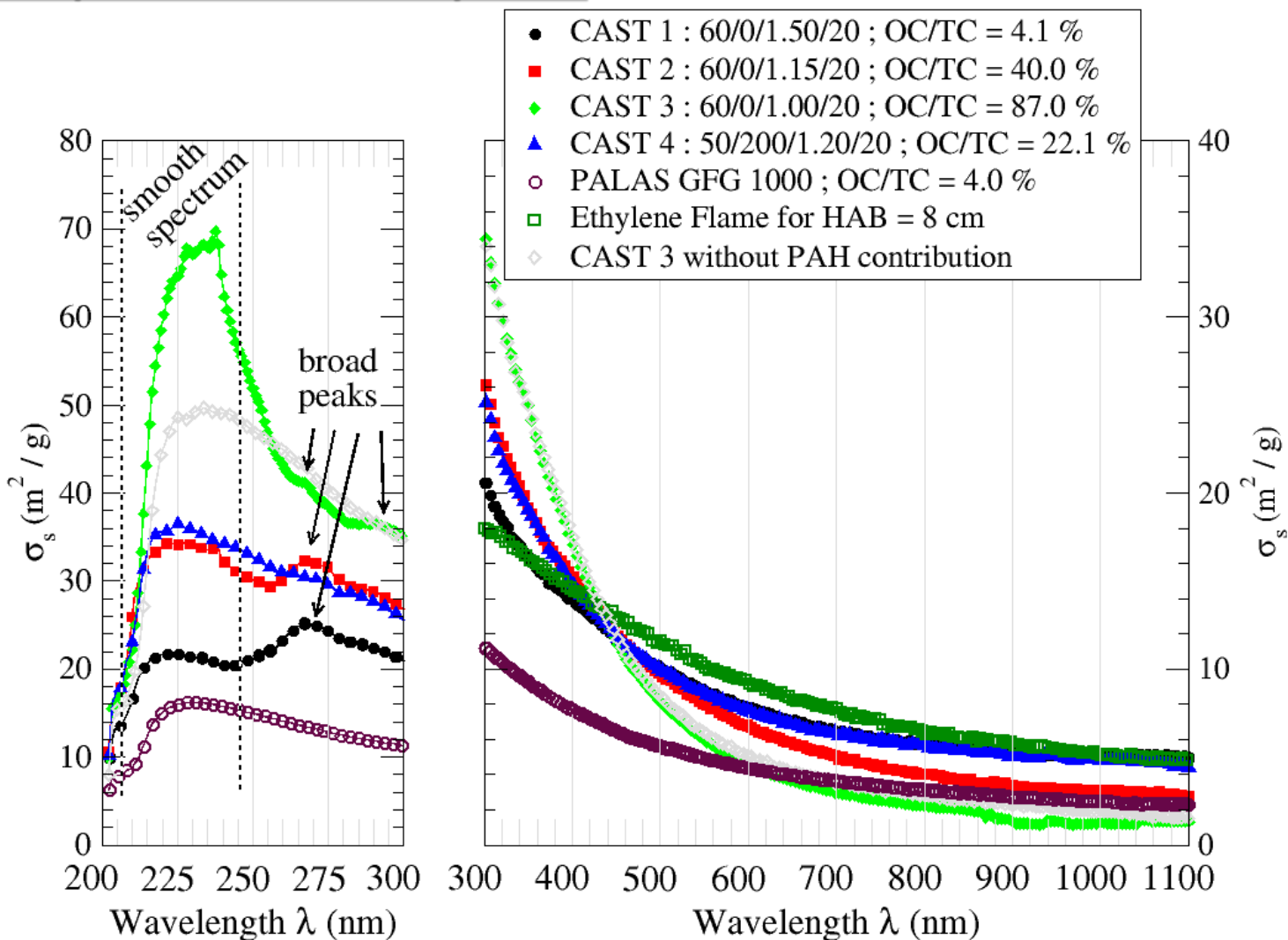
$$\sigma_s = \frac{K_{ext}}{C_s} = \frac{(C_{abs} + C_{scat})N}{\rho_{pp}f_v} = \underbrace{\frac{6\pi}{\rho_{pp}\lambda} \frac{[h(\kappa\lambda, N_p)]N_p}{\bar{N}_p} E(m)}_{\text{absorption component}} + \underbrace{\frac{24\pi^3 V_p}{\rho_{pp}\lambda^4} \frac{N_p^2 [A(\kappa\lambda, N_p)]g(R_g, \lambda, d_f)}{\bar{N}_p} F(m)}_{\text{scattering component}}$$

$$E(m) = \text{Im} \left(\frac{m^2 - 1}{m^2 + 2} \right)$$

$$F(m) = \left| \frac{m^2 - 1}{m^2 + 2} \right|^2$$

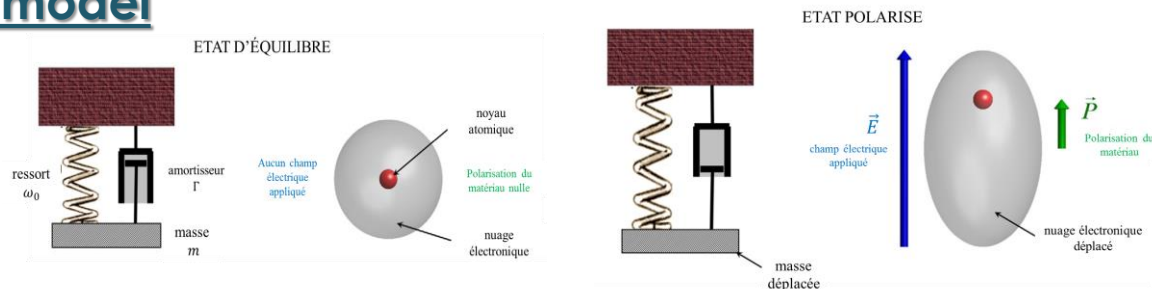
Soot optical index

Examples of Specific Extinction spectra



Soot optical index

Lorentz-Drude model



(a) Equilibrium

(b) Polarized state

$$n^2 - k^2 = 1 - \frac{e^2}{m^* \varepsilon_0} \frac{n_c}{\omega^2 + g_c^2} + \frac{e^2}{m_v \varepsilon_0} \sum_{j=1}^{N=2} \frac{n_j (\omega_{0j}^2 - \omega^2)}{(\omega_{0j}^2 - \omega^2)^2 + \omega^2 g_j^2}$$

$$2nk = \frac{e^2}{m^* \varepsilon_0} \frac{n_c g_c}{\omega(\omega^2 + g_c^2)} + \frac{e^2}{m_v \varepsilon_0} \sum_{j=1}^{N=2} \frac{n_j (\omega_j^2 - \omega^2)}{(\omega_j^2 - \omega^2)^2 + \omega^2 g_j^2}$$

Researched parameters : the total electron density n_t , the number density of bound electrons for the first oscillator n_1 , and the bound electron damping constant for the first and second oscillator g_1 and g_2 , the bound electron frequency for the second oscillator ω_2 .

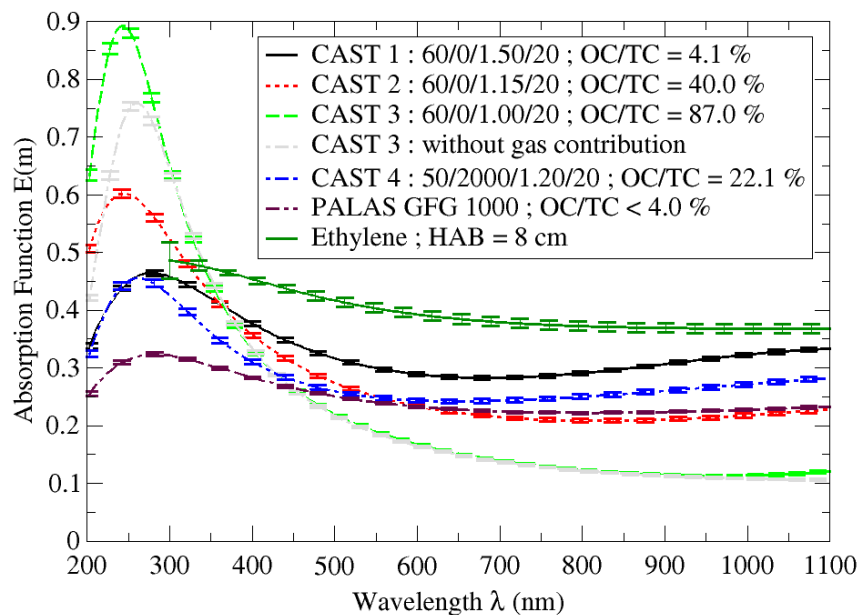
The other parameters of the Drude–Lorentz model are fixed

$$(n_c = 1.0 \times 10^{25} m^{-3}; \omega_1 = 1.25 \times 10^{15} s^{-1}, g_c = 5.4 \times 10^{14} s^{-1}).$$

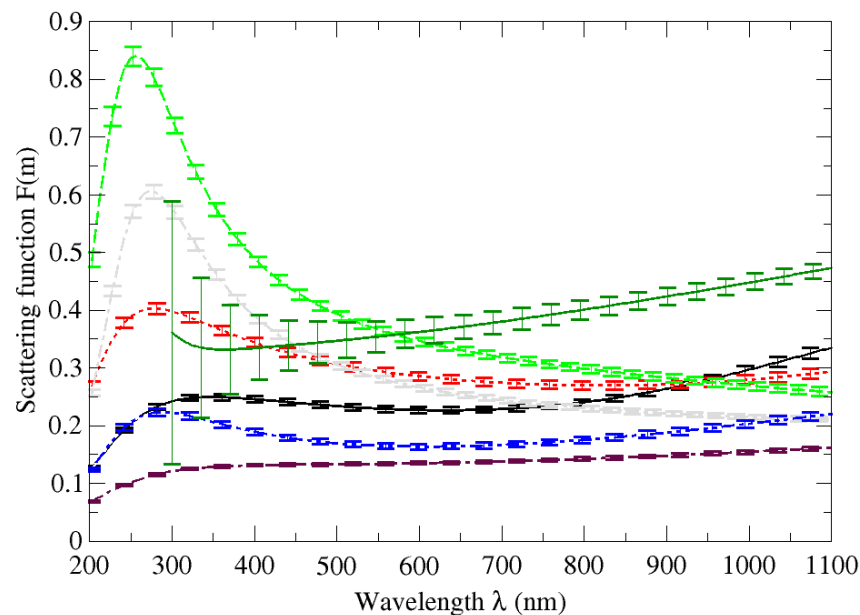
Soot optical index

Result of the inversion

$$\sigma_s = \underbrace{\frac{6\pi}{\rho_{pp}\lambda} \frac{[h(\kappa\lambda, N_p)] N_p}{\overline{N_p}} E(m)}_{\text{absorption component}} + \underbrace{\frac{24\pi^3 V_p}{\rho_{pp}\lambda^4} \frac{N_p^2 [A(\kappa\lambda, N_p)] g(R_g, \lambda, d_f)}{\overline{N_p}} F(m)}_{\text{scattering component}}$$



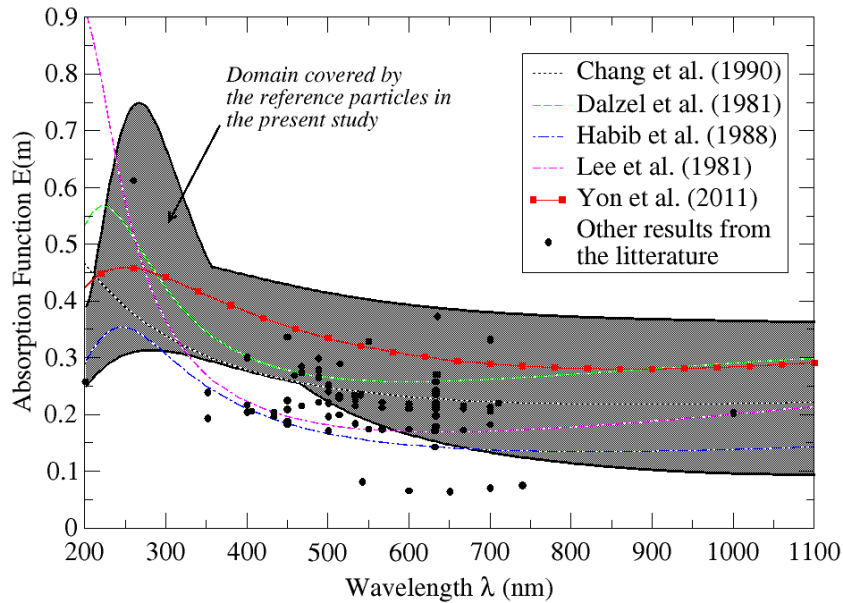
(a) Absorption function $E(m)$



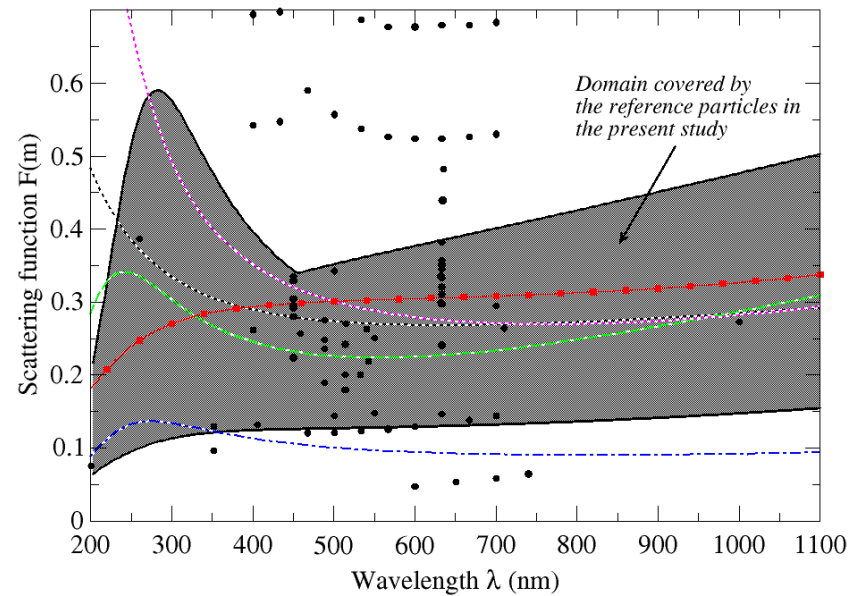
(b) Scattering function $F(m)$

Results : Application to CAST soot and to other sources

Specific extinction inversion results



(a) Absorption function $E(m)$



(b) Scattering function $F(m)$

Comparison of the domain covered by absorption and scattering function with previous results from the literature.

Conclusion

- A few examples of coupling of optical and non optical diagnostics have been presented.
- Each one depends on different properties of soot particles.
- Only the coupling of different techniques permits to envisage a “complete” characterization of soot particles.
- Optical diagnostics are very promising for an in-situ characterization of soot particles.

Thanks for your attention,

any questions ?

Application this afternoon !